

THE VERY LARGE ARRAY OBSERVATIONAL STATUS SUMMARY

Edited by J.S. Ulvestad, R.A. Perley, & G.B. Taylor

August 13, 2007

Contents

| | | |
|----------|--|----------|
| 1 | INTRODUCTION | 2 |
| 1.1 | Purpose of Document | 2 |
| 1.2 | EVLA Project and Transition | 2 |
| 2 | AN OVERVIEW OF THE VLA | 2 |
| 3 | PERFORMANCE OF THE VLA | 4 |
| 3.1 | Resolution | 4 |
| 3.2 | Sensitivity | 5 |
| 3.3 | EVLA Frequency Bands and Tunability | 9 |
| 3.4 | Elevation Effects | 10 |
| 3.5 | Field of View | 13 |
| 3.5.1 | Primary Beam | 13 |
| 3.5.2 | Chromatic Aberration (Bandwidth Smearing) | 14 |
| 3.5.3 | Time-Averaging Loss | 14 |
| 3.5.4 | Non-Coplanar Baselines | 14 |
| 3.6 | Time Resolution | 15 |
| 3.7 | Radio-Frequency Interference | 16 |
| 3.8 | Antenna Pointing | 19 |
| 3.9 | Subarrays | 20 |
| 3.10 | Positional Accuracy | 21 |
| 3.11 | Limitations on Imaging Performance | 21 |
| 3.11.1 | Image Fidelity | 21 |
| 3.11.2 | VLA-EVLA Closure Errors | 21 |
| 3.11.3 | Invisible Structures | 22 |
| 3.11.4 | Poorly Sampled Fourier Plane | 22 |
| 3.11.5 | Sidelobes from Confusing Sources | 22 |
| 3.11.6 | Sidelobes from Strong Sources | 22 |
| 3.12 | Calibration and the Flux Density Scale | 22 |
| 3.13 | Phase Calibration | 24 |
| 3.13.1 | General Guidelines for Phase Calibration | 24 |
| 3.13.2 | Rapid Phase Calibration and the Atmospheric Phase Interferometer (API) | 24 |
| 3.14 | Polarization | 25 |
| 3.15 | Spectral Line Modes | 26 |
| 3.16 | VLBI Observations | 28 |
| 3.17 | Snapshots | 28 |
| 3.18 | Shadowing and Cross-Talk | 29 |
| 3.19 | Combining Configurations and Mosaicing | 29 |
| 3.20 | Pulsar Observing | 29 |

| | | |
|----------|---|-----------|
| 3.21 | Observing High Flux Density Sources – Special Corrections | 29 |
| 3.22 | Using VLA and EVLA Antennas Together | 29 |
| 4 | USING THE VLA | 30 |
| 4.1 | Obtaining Observing Time on the VLA | 30 |
| 4.2 | Rapid Response Science | 30 |
| 4.3 | Data Analysts and General Assistance | 31 |
| 4.4 | Observing File Preparation | 31 |
| 4.5 | Fixed Date and Dynamic Scheduling | 32 |
| 4.6 | The Observations and Remote Observing | 32 |
| 4.7 | Data Processing | 32 |
| 4.8 | Travel Support for Visiting the AOC and VLA | 32 |
| 4.9 | Student Assistance for Data Reduction Visits to the AOC | 33 |
| 4.10 | Real-Time Observing | 33 |
| 4.11 | Computing at the AOC | 33 |
| 4.12 | Reservations for VLA and/or AOC | 33 |
| 4.13 | Staying in Socorro | 34 |
| 4.14 | Help for Visitors to the VLA and AOC | 34 |
| 4.15 | VLBI Remote Observing | 34 |
| 4.16 | On-Line Information about the NRAO and the VLA | 34 |
| 5 | MISCELLANEOUS | 34 |
| 5.1 | VLA Archive Data | 34 |
| 5.2 | Publication Guidelines | 35 |
| 5.2.1 | Acknowledgement to NRAO | 35 |
| 5.2.2 | Dissertations | 35 |
| 5.2.3 | Preprints | 35 |
| 5.2.4 | Reprints | 35 |
| 5.2.5 | Page Charge Support | 35 |
| 6 | DOCUMENTATION | 36 |
| 7 | KEY PERSONNEL | 37 |
| 8 | Acknowledgments | 37 |

List of Tables

| | | |
|----|--|----|
| 1 | A Possible Long Term VLA Configuration Schedule | 3 |
| 2 | Configuration Properties | 5 |
| 3 | VLA Sensitivity in Mid-2007 | 7 |
| 4 | Sensitivity Ranges of VLA Bands | 8 |
| 5 | Tuning Ranges of EVLA Bands | 11 |
| 6 | Average Power Gain Coefficients for the VLA Antennas | 11 |
| 7 | Average Inverse Voltage Gain Coefficients for the VLA Antennas | 12 |
| 8 | Reduction in Peak Response Due to Bandwidth Smearing | 14 |
| 9 | Loss vs. Averaging Time for Time Averaging Smearing | 15 |
| 10 | VLA RFI Between 1260 and 1740 MHz | 18 |
| 11 | Recommended Center Frequency/Bandwidth Combinations for L band | 18 |
| 12 | Jobserve Names of L band ‘Standard Frequencies’ | 19 |
| 13 | Flux Densities (Jy) of Standard Calibrators for November 2001 | 23 |
| 14 | Available Bandwidths and Numbers of Spectral Line Channels in Normal Mode | 26 |
| 15 | Available Bandwidths and Numbers of Spectral Line Channels in Hanning Smoothing Mode | 27 |

| | | |
|----|-----------------------------|----|
| 16 | Key VLA Personnel | 37 |
|----|-----------------------------|----|

List of Figures

| | | |
|---|---|----|
| 1 | System Temperatures vs. Frequency at K and Q Bands | 8 |
| 2 | VLA Sensitivity Between 1150 and 1250 MHz | 9 |
| 3 | EVLA Receiver Deployment Plan | 10 |
| 4 | System Temperature Variations with Elevation at L, K, and Q Bands | 12 |
| 5 | EVLA System Temperature Variation with Elevation at L Band | 13 |
| 6 | Typical L-band Interference Spectrum | 16 |
| 7 | Typical P-band Interference Spectrum | 17 |

1 INTRODUCTION

1.1 Purpose of Document

This document summarizes the current instrumental status of the Very Large Array. It is intended as a ready reference for those contemplating use of the VLA for their astronomical research. The information is in summary form – those requiring greater detail should consult the VLA’s staff members, listed in Section 7, or refer to the manuals and documentation listed in Section 6. Most of the information contained here, and much more, is available on the Web, and can be accessed through the VLA home page information for astronomers, at <http://www.vla.nrao.edu/astro/>. A companion document for the VLBA is also available from <http://www.vlba.nrao.edu/astro/>.

The Very Large Array is a large and complex modern instrument. It cannot be treated as a ‘black box’, and some familiarity with the principles and practices of its operation is necessary before efficient use can be made of it. Although the NRAO strives to make using the VLA as simple as possible, users must be aware that proper selection of observing mode and calibration technique is often crucial to the success of an observing program. Inexperienced and first-time users are especially encouraged to enlist the assistance of an experienced colleague or NRAO staff member for advice on, or direct participation in, an observing program. Refer to Section 4.14 for details. The VLA is an extremely flexible instrument, and we are always interested in imaginative and innovative ways of using it.

1.2 EVLA Project and Transition

A project that will modernize the VLA electronics systems and improve all key observational parameters by a factor of 10 is under way. Details of this Expanded VLA (EVLA) Project may be found on the web, at <http://www.aoc.nrao.edu/evla/>.

During the entire VLA Expansion Project we are committed to keeping the VLA observing and producing forefront science. It is expected, however, that there will be some periods when the amount of observing time is reduced, and the average number of antennas available may be fewer than for the nominal VLA. To keep people informed of the impact of the EVLA construction on VLA observations we maintain a web site at: <http://www.aoc.nrao.edu/evla/archive/transition/impact.html>. At the web site are short-, medium- and long-term forecasts. Users should consult these forecasts before proposing for time or observing with the VLA.

We now are returning retrofitted EVLA antennas to the VLA to be used as part of normal VLA observations. These antennas have new feed systems, wideband electronics, and fiber-optic data transmission systems; their data are “translated” (and reduced) considerably to be correlated against VLA antennas in the VLA correlator. Although we have put considerable effort into making it possible to observe with mixed arrays of VLA and EVLA antennas, fundamental hardware differences (e.g., mismatched bandpasses) lead to a number of complications, which often must be taken into account in constructing observing programs or in analyzing data. Although some information is provided in this document about observations using VLA+EVLA antennas, details change frequently; up-to-date information is provided at <http://www.vla.nrao.edu/astro/guides/evlareturn/>, and *must* be consulted before VLA observations are undertaken.

2 AN OVERVIEW OF THE VLA

The VLA is a 27-element interferometric array which will produce images of the radio sky at a wide range of frequencies and resolutions. The basic data produced by the array are the visibilities, or measures of the spatial coherence function, formed by correlation of signals from the array’s elements. The most common mode of operation uses these data, suitably calibrated, to form images of the radio sky as a function of sky position and frequency. Another mode of observing (commonly called *phased array*) allows operation of the array as a single element through coherent summation of the individual antenna signals. This mode is commonly used for VLBI observing and for observations of rapidly varying objects, such as pulsars.

The VLA can vary its resolution over a range exceeding a factor of ~ 50 through movement of its component antennas. There are four basic arrangements, called configurations, whose scales vary by the ratios 1 : 3.2 : 10 : 32 from smallest to largest. These configurations are denoted **D**, **C**, **B**, and **A** respectively. In addition, there are 3 ‘hybrid’ configurations labelled **DnC**, **CnB**, and **BnA**, in which the North arm antennas are deployed in the next larger configuration than the SE and SW arm antennas. These hybrid configurations are especially well suited for observations of sources south of $\delta = -15^\circ$ or north of $\delta = +75^\circ$.

Beginning in 1998, the standard **C** configuration was replaced by a slightly modified one, formerly known as **CS**, in which one antenna from the middle of the north arm (N10) is placed at N1 (at the center of the array) to give better short-spacing baseline coverage. See VLA Scientific Memos # 172 and 175, available from Reference 12 (see Section 6).

Traditionally, the VLA has completed one cycle through all four configurations in approximately a 16 month period. However, this cycle is likely to change beginning in 2007 in order to accommodate both the EVLA commissioning and an increase in time allocated to large observing programs. In particular, the configuration schedule is likely to change based on the delivery schedule for the EVLA correlator. One possible VLA configuration schedule for the upcoming years is outlined in Table 1, but prospective users should consult the web page <http://www.vla.nrao.edu/genpub/configs/> or recent NRAO and AAS newsletters for up-to-date schedules and associated proposal deadlines. Refer to Section 4.1 for information on how to submit an observing proposal.

Table 1: **A Possible Long Term VLA Configuration Schedule**

| | Q1 | Q2 | Q3 | Q4 |
|------|------------|------------|------------|------------|
| 2007 | D | D,A | A | A,B |
| 2008 | B | C | D,A | A |
| 2009 | A,D | D,C | C,B | B,A |

Note: The schedules for 2007 and 2008 are likely to change, based on pressure for large proposals, while that for 2009 depends heavily on the EVLA correlator delivery schedule.

Observing projects on the VLA vary in duration from as short as 1/2 hour to as long as several weeks. Most observing runs have durations of a few to 24 hours, with only one, or perhaps a few, target sources. However, since the VLA is a two-dimensional array, images can be made with data durations of less than one minute. This mode, commonly called *snapshot* mode, is well suited to surveys of relatively strong, isolated objects. See Section 3.17 for details.

The VLA can be broken into as many as five sub-arrays, each of which can observe a different object at a different band. This is especially useful for multi-band flux density monitoring observations, and for observing compact objects for which the VLA’s full imaging capability and sensitivity are not required. However, important restrictions apply when multiple sub-arrays are used – refer to Section 3.9 for these restrictions.

All VLA antennas are permanently outfitted with receivers for seven wavelength bands centered near $\lambda\lambda$ 90, 20, 6, 3.6, 2.0, 1.3, and 0.7 cm. These bands are commonly referred to as P, L, C, X, U, K and Q bands, respectively. However, the staging of the EVLA antenna retrofits is such that the EVLA antennas have the old U band systems removed, and they will not be replaced with new wideband systems until 2010 and later. Thus, the maximum number of antennas with U band available will decrease monotonically from approximately 20 at the beginning of 2007 to approximately 14 at the beginning of 2008. In addition, a new receiving system centered near λ 1.0 cm (32 GHz) will begin to be implemented on EVLA antennas in 2007, but a significant number of antennas will not have this observing band until the end of 2007. See Section 3.3 for more details about the availability of new bands and enhanced frequency tunability for EVLA antennas.

The ‘4-band’ system (better known as the 74 MHz system) is now available on all antennas, but is not permanently installed. The long dipoles needed to efficiently illuminate the antennas have been shown to reduce the gain and increase the system temperature at 20 cm by about 5%. Because of this, and the experimental nature of this frequency band, we will continue past practice

of mounting the dipoles for limited periods of time during which 74 MHz observing is concentrated. At present, this means that, provided a sufficient number of project hours at 74 MHz have been approved, dipoles are mounted near the end of the **A** configuration for observations in the **A**, **BnA** and **B** configurations. Typically, there has not been sufficient proposal pressure to mount the dipoles in the more compact VLA configurations, although a special observing session for **CnB** and **C** configurations is being carried out in late 2006. The dipoles are removed after observations are completed in the **B** and/or **C** configurations.

The array can tune to two different frequencies from the same wavelength band provided the frequency difference does not exceed approximately 450 MHz. Right-hand circular (RCP) and left-hand circular (LCP) polarizations are received for both frequencies. Each of these four data streams is called an ‘IF’ (for “Intermediate Frequency” channel). These four data streams are known in VLA-ese as IFs ‘A’, ‘B’, ‘C’, and ‘D’. IFs A and B receive RCP, IFs C and D receive LCP. IFs A and C are always at the same frequency, as are IFs B and D. [But the (A,C) frequency is usually different than the (B,D) frequency.] Observations at more widely separated frequencies can only be made within the same run by time switching between the frequencies. This operation takes less than 30 seconds. The array also can observe simultaneously one frequency within L band and one within P band (known as LP), or one within 4-band and one within P band (known as 4P mode). These are the only currently *supported* modes in which frequencies within two different bands can be observed simultaneously.

Observations at seven different bandwidths (given by $50/2^n$ MHz, with $n = 0, 1, \dots, 6$) are possible¹. A 200 kHz bandwidth is also available in spectral line mode. Continuum mode users wishing to use the 200 kHz bandwidth should first consult VLA staff. Different bandwidths can be used for each of the two separate frequencies. Wider bandwidths provide better sensitivity, but also increase the chromatic aberration. Refer to Section 3.5.2 for details.

The VLA correlator has two basic modes, *Continuum* and *Spectral Line*. In *Continuum mode*, the correlator provides the four correlations (RR, RL, LR, LL) needed for full polarimetric imaging at both frequencies. This mode is particularly well suited to high sensitivity, narrow field-of-view projects. The *Spectral Line mode* is a spectrum-measuring mode principally intended for observing spectral lines. There are many options allowed in this mode. Besides its use for all spectral line projects, certain continuum projects which require extremely high dynamic range, or large field-of-view at high spatial resolution, will benefit from use of this mode. (These are sometimes referred to as *multichannel continuum* or *pseudo-continuum* projects.) This mode also is used to great advantage when RFI (Radio Frequency Interference) is expected within the bandpass. The Spectral Line modes are further described in Section 3.15.

3 PERFORMANCE OF THE VLA

This section contains details of the VLA’s resolution, sensitivity, tuning range, dynamic range, pointing accuracy, and modes of operation. Detailed discussions of most of the observing limitations are found elsewhere. In particular, see References 1 and 2, listed in Section 6.

3.1 Resolution

The VLA’s resolution is generally diffraction-limited, and thus is set by the array configuration and frequency of observation. It is important to be aware that a synthesis array is ‘blind’ to structures on angular scales both smaller and larger than the range of fringe spacings given by the antenna distribution. For the former limitation, the VLA acts like any single antenna – structures smaller than the diffraction limit ($\theta \sim \lambda/D$) are broadened to the resolution of the antenna. The latter limitation is unique to interferometers – it means that structures on angular scales significantly larger than the fringe spacing formed by the shortest baseline are not measured. No subsequent processing can fully recover this missing information, which can only be obtained by observing in

¹The VLA’s maximum bandwidth is commonly referred to as 50 MHz per IF, but the actual effective bandwidth is closer to 43 MHz, due to bandpass roll-off.

a smaller array configuration, using the mosaicing method, or with an instrument (such as a large single antenna) which provides this information.

Table 2 summarizes the relevant information. This table shows the maximum and minimum antenna separations, the approximate synthesized beam size (full width at half-power), and the scale at which severe attenuation of large scale structure occurs.

A project with the goal of doubling the longest baseline available in the **A** configuration by establishing a real-time fiber optic link between the VLA and the VLBA antenna at Pie Town has been completed. This link has been operational for observations taking place during **A** configuration. Due to the pressures of EVLA commissioning, the Pie Town link will not be offered during the **A** configuration session in 2007, and is unlikely to be offered in the future until/unless the link is upgraded to be compatible with EVLA characteristics.

Table 2: Configuration Properties

| Configuration | A | B | C | D |
|-------------------------|--|----------|--------------------|----------|
| $B_{\max}(\text{km}^1)$ | 36.4 | 11.4 | 3.4 | 1.03 |
| $B_{\min}(\text{km}^1)$ | 0.68 | 0.21 | 0.035 ⁵ | 0.035 |
| | Synthesized Beamwidth θ_{HPBW} (arcsec) ^{1,2,3} | | | |
| 400 cm | 24.0 | 80.0 | 260.0 | 850.0 |
| 90 cm | 6.0 | 17.0 | 56.0 | 200.0 |
| 20 cm | 1.4 | 3.9 | 12.5 | 44.0 |
| 6 cm | 0.4 | 1.2 | 3.9 | 14.0 |
| 3.6 cm | 0.24 | 0.7 | 2.3 | 8.4 |
| 2 cm | 0.14 | 0.4 | 1.2 | 3.9 |
| 1.3 cm | 0.08 | 0.3 | 0.9 | 2.8 |
| 0.7 cm | 0.05 | 0.15 | 0.47 | 1.5 |
| | Largest Angular Scale θ_{LAS} (arcsec) ^{1,4} | | | |
| 400 cm | 800.0 | 2200.0 | 20000.0 | 20000.0 |
| 90 cm | 170.0 | 540.0 | 4200.0 | 4200.0 |
| 20 cm | 38.0 | 120.0 | 900.0 | 900.0 |
| 6 cm | 10.0 | 36.0 | 300.0 | 300.0 |
| 3.6 cm | 7.0 | 20.0 | 180.0 | 180.0 |
| 2 cm | 4.0 | 12.0 | 90.0 | 90.0 |
| 1.3 cm | 2.0 | 7.0 | 60.0 | 60.0 |
| 0.7 cm | 1.3 | 4.3 | 43.0 | 43.0 |

These estimates of the synthesized beamwidth are for a uniformly weighted, untapered map produced from a full 12 hour synthesis observations of a source which passes near the zenith.

Footnotes:

1. B_{\max} is the maximum antenna separation, B_{\min} is the minimum antenna separation, θ_{HPBW} is the synthesized beam width (FWHM), and θ_{LAS} is the largest scale structure ‘visible’ to the array.
2. The listed resolutions are appropriate for sources with declinations between -15 and 75 degrees. For sources outside this range, the extended north arm hybrid configurations (**BnA**, **CnB**, **DnC**) should be used, and will provide resolutions similar to the smaller configuration of the hybrid, except for declinations south of -30 . No double-extended north arm hybrid configuration (e.g., **CnA**, or **DnB**) is provided.
3. The approximate resolution for a naturally weighted map is about 1.5 times the numbers listed for θ_{HPBW} . The values for snapshots are about 1.3 times the listed values.
4. The largest angular scale structure is that which can be imaged reasonably well in full synthesis observations. For single snapshot observations the quoted numbers should be divided by two.
5. The standard **C** configuration has been replaced by a slightly modified one, formerly known as **CS**, wherein an antenna from the middle of the north arm has been moved to the central pad ‘N1’. This results in improved imaging for extended objects, but will degrade snapshot performance. Although the minimum spacing is the same as in **D** configuration, the surface brightness sensitivity to extended structure is considerably inferior to that of the **D** configuration (but considerably better than standard **C** configuration).

3.2 Sensitivity

Table 3 shows the VLA sensitivities expected for natural weighting of the visibility data. The values listed are the expected rms fluctuations due to thermal noise on an image, calculated using the

standard formulae with the system temperatures and efficiencies listed. A maximum number of 25 antennas is used in these calculations (except for U band); at any given time, it is assumed that 3 of the possible 28 antennas are missing, one each for EVLA mechanical retrofitting, EVLA electronics outfitting, and EVLA commissioning. The tabulated sensitivity values are realized in practice except at low frequencies and in smaller configurations where the sensitivities are limited by confusing sidelobes from objects outside the image. The rms limit due to confusing sources for the VLA in **D** configuration is estimated in Table 3. Another case where the thermal rms noise will not be achieved is in imaging very bright objects where the residual image noise is due to baseline dependent errors (‘closure errors’ – see 3.11).

In general, the expected point-source rms noise in mJy on an output image, for natural weighting, can be calculated with the following formula:

$$\Delta I_m = \frac{K}{\sqrt{N(N-1)(N_{\text{IF}}T_{\text{int}}\Delta\nu_{\text{M}})}} \text{ mJy} \quad (1)$$

where N is the number of antennas, T_{int} is the total on-source integration time in hours, $\Delta\nu_{\text{M}}$ is the effective continuum bandwidth or spectral-line channel width in MHz, and N_{IF} is the number of IFs (from 1 to 4) or spectral line channels (from 1 to 512) which will be combined in the output image². K is a system constant, equal to 1000, 50, 8.0, 7.8, 6.6, 27, 14, and 35³ for 4, P, L, C, X, U, K, and Q bands respectively. This constant K also can be expressed in terms of system temperature and efficiency as:

$$K = \frac{0.12T_{\text{sys}}}{\eta_a} \quad (2)$$

where T_{sys} is the system temperature, and η_a is the antenna efficiency, as listed in Table 3. (A correlator efficiency of 0.78 has already been incorporated into this expression). For the more commonly used uniform weighting employing the robust weight scheme intermediate between pure natural and pure uniform weightings (available in the AIPS task **IMAGR**), the sensitivity will be a factor of about 1.2 worse than the listed values. To aid VLA proposers there is an exposure tool calculator on-line at <http://www.vla.nrao.edu/astro/guides/exposure/> that provides a graphical user interface to these equations.

It is important to note that these listed sensitivities are calculated from data taken in optimum conditions. For many bands, the system temperature and gain are significant functions of elevation and weather conditions (see next section).

A useful alternate form of the point-source sensitivity equation, for 25 identical antennas, is

$$\Delta I_m = \frac{45.9K}{\sqrt{N_{\text{pts}}N_{\text{IF}}\Delta t_{\text{int}}\Delta\nu_{\text{M}}}} \text{ mJy} \quad (3)$$

where N_{pts} is the number of visibility points (which is listed in the AIPS header), and Δt_{int} is the integration time per visibility in seconds. N_{IF} , $\Delta\nu_{\text{M}}$ and K are defined as above. For 16 antennas, a typical number available at U band, the numerical coefficient should be changed from 45.9 to 72.5.

The limiting brightness temperature achievable by an array is a complicated function of the source distribution and array configuration. However, for the simplified case of an object approximately the size of the synthesized beam, the following relation between brightness temperature and flux density can be applied:

$$T_{\text{b}} = F \cdot S \quad (4)$$

where T_{b} is the brightness temperature (Kelvins) corresponding to S mJy per beam, and F is a constant depending only upon array configuration: $F = 300, 30, 3, 0.3$ for **A**, **B**, **C**, and **D** configurations, respectively. The limiting brightness temperature can be obtained by substituting the rms noise, ΔI_m , for S . A more detailed description of the relation between flux density and surface brightness is given in Chapter 7 of Reference 1, listed in Section 6.

²For most continuum observations, N_{IF} will be either 4 (all IFs), or 2 (one IF pair), and $\Delta\nu_{\text{M}}$ will be the IF bandwidth. Thus, $N_{\text{IF}} = 2$ for Stokes’ Q, U and (true) I images at a single frequency. For spectral line work, $\Delta\nu_{\text{M}}$ is the spectral resolution (channel width) in MHz.

³The quoted value of K for Q-band assumes a dry and stable atmosphere, and excellent pointing characteristics.

Table 3: VLA Sensitivity in Mid-2007

| Frequency (GHz) | Band Name | | System Temperature ¹ (K) | Antenna Efficiency ² (%) | Number Antennas (VLA+EVLA) | RMS (10 min) Sensitivity (mJy) |
|--------------------|---------------------------|--|---|--|--|---|
| | Approximate Wavelength | Letter Code | | | | |
| 0.073 - 0.0745 | 400 cm | 4 | 1000-10000 | 15 | 16+9 | 160 ⁽³⁾ |
| 0.3 - 0.34 | 90 cm | P | 150-180 | 40 | 16+9 | 1.5 ⁽³⁾ |
| 1.24 - 1.70 | 20 cm | L | 35 | 55 | 16+9 | 0.061 |
| 4.5 - 5.0 | 6 cm | C | 45 | 69 | 16+9 | 0.058 |
| 8.1 - 8.8 | 3.6 cm | X | 35 | 63 | 16+9 | 0.049 |
| 14.6 - 15.3 | 2 cm | U | 120 | 58 | 16+0 | 0.32 |
| 22.0 - 24.0 | 1.3 cm | K | 50 - 80 | 40 | 16+9 | 0.11 ⁽⁴⁾ |
| 40.0 - 50.0 | 0.7 cm | Q | 80 | 35 | 16+9 | 0.27 ⁽⁵⁾ |
| Frequency (GHz) | Wavelength | RMS Point-Source Sensitivity (12 hours) (mJy) | Untapered Brightness Sensitivity ⁽⁶⁾ (D-config) (mKelvins) | Antenna Primary Beam Size (FWHP) θ_{PB} | Peak/Total Confusing Source in Beam (Jy) | RMS Confusion Level (D-config) (μ Jy/beam) |
| 0.073 - 0.0745 | 400 cm | 17 ⁽³⁾ | 2000 | 700' | 20/350 | lots |
| 0.3 - 0.34 | 90 cm | 0.18 ⁽³⁾ | 21.3 | 150' | 1.8/15 | 4400 |
| 1.24 - 1.70 | 20 cm | 0.0071 | 0.8 | 30' | 0.11/0.35 | 86 |
| 4.5 - 5.0 | 6 cm | 0.0069 | 0.8 | 9' | 0.002 | 3.6 |
| 8.1 - 8.8 | 3.6 cm | 0.0057 | 0.6 | 5.4' | 0.001 | 0.89 |
| 14.6 - 15.3 | 2 cm | 0.037 | 4.4 | 3' | 0.0001 | 0.12 |
| 22.0 - 24.0 | 1.3 cm | 0.013 ⁽⁴⁾ | 1.5 | 2' | 0.00001 | — |
| 40.0 - 50.0 | 0.7 cm | 0.032 ⁽⁵⁾ | 3.8 | 1' | — | — |

All sensitivity calculations assume 43 MHz bandwidth per IF, (except for P-band and 4-band, where 3.125 MHz and 0.78 MHz are used), two IF pairs (four IFs), natural weighting, and an elevation of 45 degrees. Sixteen VLA and nine EVLA antennas are assumed, as will be the case in the period near April-June 2007; there will be no EVLA antennas with 2 cm (U band) installed. EVLA antennas are assumed to have the same performance as VLA antennas, although they will be significantly better at some bands (particularly at 6 cm = C band); since we mostly have “transition” EVLA receivers at present, the final system temperatures are not yet available. Performance will degrade for large zenith angles at high frequencies and for sources close to the galactic plane at low frequencies. The confusion limits (see Condon 2002, ASP Conf. 278, p. 155) for C configuration are approximately a factor of 10 less than those tabulated above for D configuration.

Footnotes:

1. Temperature ranges listed at P, K, and Q bands include sky temperature variations due to the galactic plane (P-band) or Earth’s atmosphere (K and Q bands). System temperatures for VLA antennas at L band are increased substantially at elevations below 45° due to ground pickup; this effect is considerably reduced (though not completely eliminated) in the EVLA antennas because of their larger L band feeds.
2. This is the system efficiency without the correlator factor (about 0.78). Efficiencies at U, K, and Q bands at low elevations (< 30 degrees) are considerably decreased due to gravitational distortions of the antenna figure.
3. Values listed assume observations near the galactic poles, and ‘3-D’ imaging. Snapshot observations will not usually reach this level, as the confusion problem is insoluble with only snapshot u,v coverage. Full-beam A configuration deconvolution at 74 MHz will be calibration-limited due to the non-isoplanatic ionosphere.
4. Listed sensitivity is for El = 45° and very dry atmosphere at 22 GHz. A wet atmosphere can increase zenith opacity from 5 to 15 percent, and increase the sky temperature from 10 to 40 K.
5. Listed sensitivity is for El = 45° and dry atmosphere at 43 GHz. A wet atmosphere can increase zenith opacity from 6 to 8 percent, and increase the zenith sky temperature from 15 to 24 K. Atmospheric attenuation and temperature increase dramatically with increasing frequency – sky temperatures exceeding 55 K and zenith opacity of 25 percent are expected at 49 GHz.
6. Values listed assume a Gaussian object with the same size as the synthesized beam in D configuration. Since natural weighting is assumed, the beam sizes are ~50% larger in each dimension than the values given in Table 2. Realistic objects will always have a higher brightness temperature limit – roughly increasing in proportion to the number of synthesized beams (in two dimensions) across the source.

For observers interested in HI in galaxies, a number of interest is the sensitivity of the observation to the HI mass. This is given by van Gorkom et al. (1986; AJ, 91, 791):

$$M_{\text{HI}} = 2.36 \times 10^5 D^2 \sum S \Delta V M_{\odot} \quad (5)$$

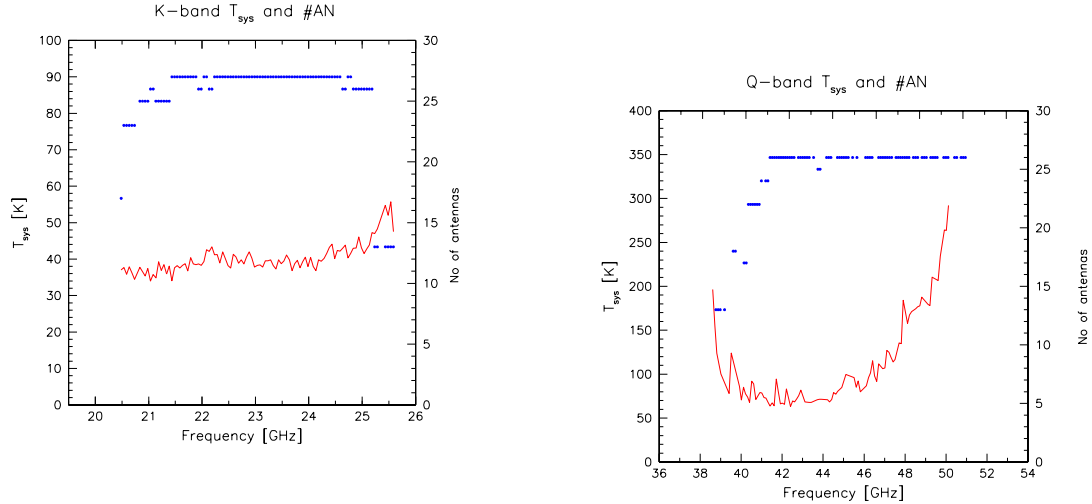


Figure 1: **System Temperatures vs. Frequency at K and Q bands.** Above are plots of the system temperature (solid red line) versus observing frequency at K and Q bands. The data were taken during night time in May 2003, under very good weather conditions. This plot shows that the system temperature is stable across the band. In blue is the number of antennas that successfully locked at the given frequency.

Table 4: **Sensitivity Ranges of VLA Bands**

| Band | 0.9 x Nominal | 0.5 x Nominal | Extreme Range |
|--------|-------------------|-------------------|-------------------|
| 90 cm | 305 - 337 MHz | 303 - 342 MHz | 298 - 345 MHz |
| 20 cm | 1240 - 1700 MHz | 1170 - 1740 MHz | 1150 - 1750 MHz |
| 6 cm | 4500 - 5000 MHz | 4250 - 5100 MHz | 4200 - 5100 MHz |
| 3.6 cm | 8080 - 8750 MHz | 7550 - 9050 MHz | 6800 - 9600 MHz |
| 2 cm | 14650 - 15325 MHz | 14250 - 15700 MHz | 13500 - 16300 MHz |
| 1.3 cm | 21200 - 25200 MHz | 20600 - 25200 MHz | 20400 - 25500 MHz |
| 0.7 cm | 40500 - 44500 MHz | 39000 - 47500 MHz | 38000 - 51000 MHz |

where D is the distance to the galaxy in Mpc, and $S\Delta V$ is the HI line area in units of Jy km/s.

The sensitivity varies across each observing band. Table 4 gives the frequency ranges for each band at which the sensitivity degrades by 10% and by a factor of two. Also included are the maximum ranges over which the VLA receivers remain operative. At these extreme ends, the system sensitivity is typically 10 to 100 times worse than at band center. Furthermore, not all antennas will operate at these frequencies. For similar information for EVLA antennas, see Section 3.3. In Figure 1, we show the system temperature and number of operable antennas plotted as a function for frequency for K and Q bands.⁴ For all bands, consider consulting a VLA staff scientist if you wish to observe near the band edges.

In view of the importance of observations at the lower edge of the 20-cm band for studies of red-shifted HI, some special words are appropriate to describe the performance of the VLA at frequencies below 1250 MHz. The roll-off of this band at the low frequency edge is very gentle, and useful observations at 1155 MHz and lower have been made. However, not all frequencies can be tuned, as tests have shown there are four 10 MHz wide ‘notches’, centered at 1212, 1182, 1162 and

⁴The number of operable antennas was determined when all antennas had old VLA electronics; the retrofitted EVLA antennas have wider tuning capabilities.

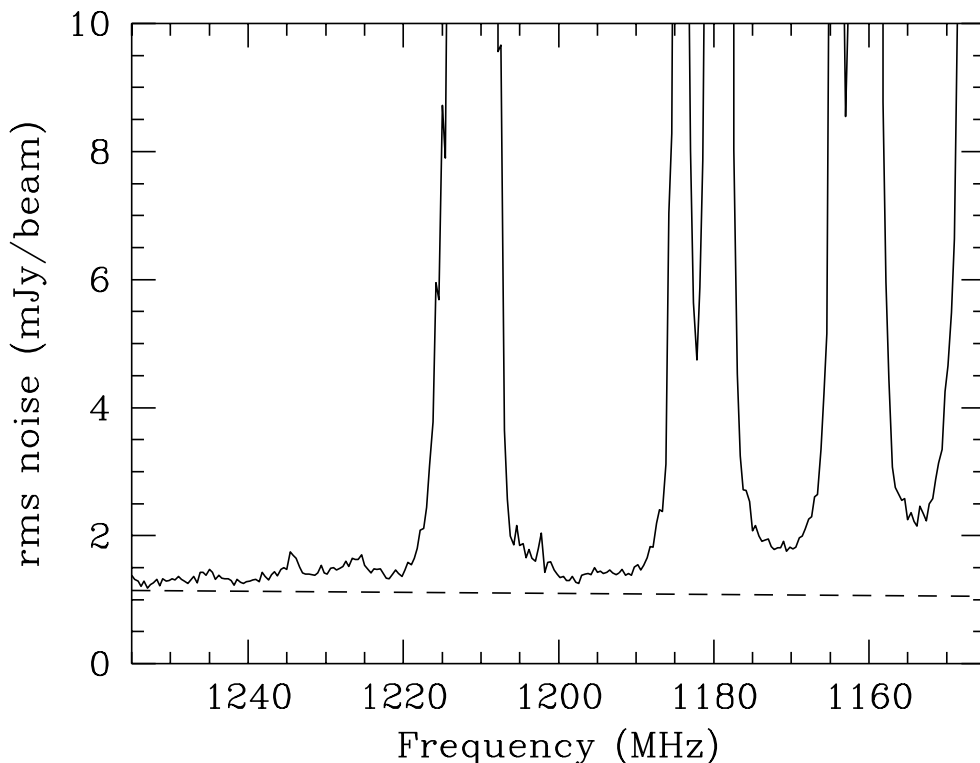


Figure 2: **VLA Sensitivity Between 1150 and 1250 MHz.** This plot shows the relative sensitivity of the VLA at the lower end of the 20 cm band. The dashed line represents the sensitivity at the center of the band, so it can be seen that serious degradation in sensitivity is not notable until below 1190 MHz. The four ‘notches’ are instrumental in origin.

1150 MHz, within which the array can take no useful data. These notches exist in both RR and LL correlations but vary in shape and central frequency from antenna to antenna. A plot of the relative sensitivity between 1150 and 1250 MHz is shown in Figure 2.

The sensitivity at the low frequency bands (90 cm and 400 cm) is difficult to parameterize. There are two important effects which limit the sensitivity.

1. The diffuse galactic background contributes an important fraction of the total system temperature – especially at 400 cm, where it is the only important contributor. This means that the sensitivity will vary by nearly a factor of 10 between locations on the galactic plane and locations near the galactic poles.
2. The primary beam at both bands is very broad, and the sidelobe levels comparatively high, resulting in significant sensitivity to objects far from the target object. Because of the difficulty in imaging very large fields of view (due to the non-coplanar baseline effect, see Section 3.5.4, and the non-isoplanicity over large angles), the sidelobes of undeconvolved objects in non-imaged areas (essentially the entire 2π steradians visible to the antennas!) will appear in the map of the target source. Use of the AIPS program `IMAGR` will permit removal of the major background objects, and should result in a sensitivity not worse than a factor of two higher than that expected on the basis of the system temperature.

3.3 EVLA Frequency Bands and Tunability

The EVLA electronics and local-oscillator systems enable tuning over wider frequencies, which is possible with the wideband feeds being installed on retrofitted antennas (or already present at K and

EVLA Receiver Schedule - Number Available at Beginning of each Calendar Year

(Based on Antenna Outfitting Plan - 28 June 2006; Assumes adequate staffing effort thru end 2012)

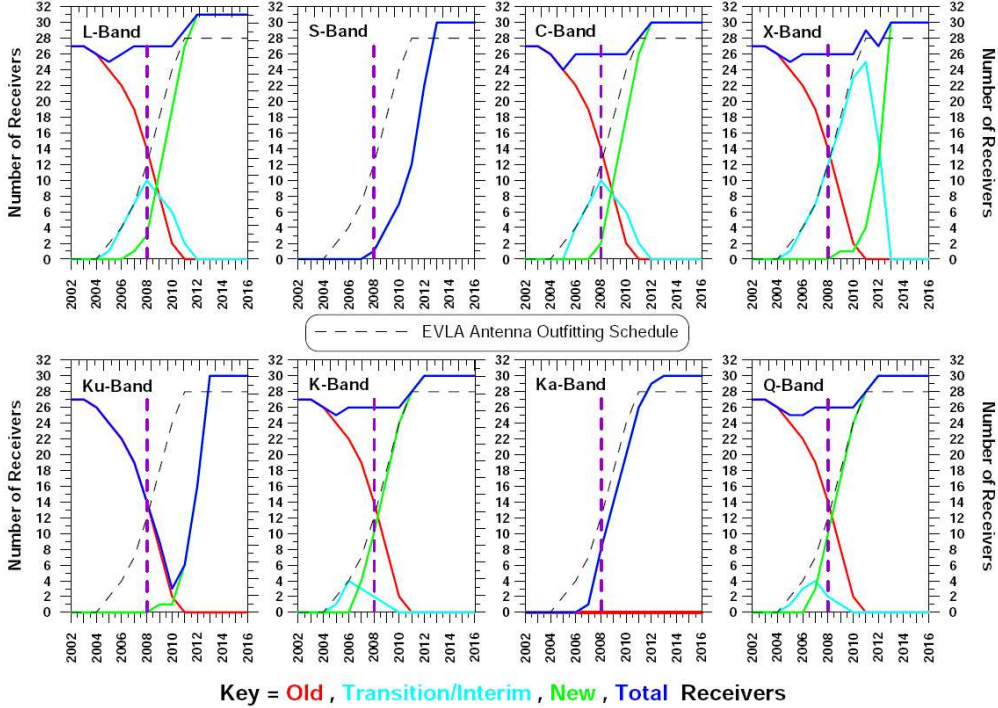


Figure 3: **EVLA Receiver Deployment Plan.** Above are plots of planned deployment schedule for the EVLA receivers until the end of the EVLA Construction Project in 2012. The eight EVLA bands are listed in separate plots, with observing frequency increasing from upper left to lower right. The decreasing red lines indicate old VLA receiver systems. The light blue lines indicate transition EVLA receivers; in the case of L, C, and X bands, these receivers have the old VLA frequency coverage rather than the more expanded EVLA frequency coverage. The green lines indicate the numbers of final EVLA receivers, and the dark blue lines indicate the total numbers of receivers. (Note that the dark blue and green lines overlap completely for the new S and Ka bands.) The vertical dashed line (in purple) indicates the beginning of 2008, after which the prototype EVLA correlator will begin to appear. Finally, the diagonal dashed line (in black), identical for each band, gives the total number of EVLA antennas that will be outfitted as a function of time. Approximate frequency coverage of the final EVLA receivers is indicated below in Table 5.

Q bands). In 2007, there will be enough EVLA antennas available to enable the first observations to make use of this wideband tuning capability, and we also will begin equipping EVLA antennas with new receiver systems at Ka band (λ 1.0 cm). For example, the new C band tuning will enable observations of methanol at 6.7 GHz, while the new K band tuning will enable observations of the 22.235 GHz H_2O line at redshifts $z = 0.1$ to $z \approx 0.18$. Figure 3 shows the present plan for EVLA receiver deployment over the remainder of the EVLA Construction Project, while Table 5 gives a prediction of the new frequency capabilities that we expect in June 2007 and December 2007.

3.4 Elevation Effects

The VLA’s antenna performance changes with elevation. These changes are significant at L, U, K, and Q bands, and must be corrected for high-precision imaging.

The loss of performance is due to two different effects:

1. The sky and ground temperature contributions to the total system temperature increase with decreasing elevation. This effect is very strong at L, K, and Q bands, as shown in Figure 4,

Table 5: **Tuning Ranges of EVLA Bands**

| Band | Range | No. EVLA Antennas Available | |
|------------|-----------------|-----------------------------|---------------|
| | | June 2007 | December 2007 |
| 20 cm (L) | 1.2 - 2.0 GHz | 2 | 3 |
| 13 cm (S) | 2.0 - 4.0 GHz | 0 | 0 |
| 6 cm (C) | 4.0 - 8.0 GHz | 1 | 2 |
| 3 cm (X) | 8.0 - 12.0 GHz | 0 | 0 |
| 2 cm (U) | 12.0 - 18.0 GHz | 0 | 0 |
| 1.3 cm (K) | 18.0 - 26.5 GHz | 7 | 11 |
| 1 cm (Ka) | 26.5 - 40.0 GHz | 4 | 9 |
| 0.7 cm (Q) | 40.0 - 50.0 GHz | 7 | 11 |

and is relatively unimportant at the other bands. The source of the excess noise at L-band is the ground itself ('spillover'), due to the microwave lens feed structure; this effect is greatly reduced in retrofitted EVLA antennas, as shown in Figure 5. At K and Q bands, the extra noise comes directly from atmospheric emission, primarily from water vapor at K-band, and from water vapor and the broad wings of the strong 63 GHz O₂ transitions at Q-band.

In general, the zenith atmospheric opacity to microwave radiation is very low – typically less than 0.01 at L and C and X bands, 0.02 at U band, 0.05 to 0.2 at K band, and 0.05 to 0.1 at the lower half of Q band, rising to 0.3 by 49 GHz. The opacity at K band displays strong variations with time of day and season, primarily due to water vapor. Conditions are best at night, and in the winter. Q band opacity, caused by O₂ in the atmosphere, is considerably less variable.

Observers should remember that clouds, especially clouds with large water droplets (read, thunderstorms!), can add appreciable noise to the system temperature. Significant increases in system temperature can, in the worst conditions, be seen at wavelengths as long as 6 cm.

2. The antenna figure degrades at low elevations, leading to diminished forward gain at the shorter wavelengths. In general, the forward power gain of the antennas can be well fitted by a simple parabola of form: $G(E) = G_0 - G_2(E - E_m)^2$, where E is the elevation (in degrees), and E_m is the elevation of maximum forward gain. The average coefficients G_0 , G_2 , and E_m are given in Table 6. The gain-elevation effect is negligible at frequencies below 8 GHz.

Table 6: **Average Power Gain Coefficients for the VLA Antennas**

| Band | G_0 | G_2 | E_m |
|------|-------|----------------------|-------|
| Q | 1.00 | 3.0×10^{-4} | 50 |
| K | 1.00 | 1.5×10^{-4} | 58 |
| U | 1.00 | 3.6×10^{-5} | 46 |
| X | 1.00 | 0.7×10^{-5} | 50 |

These power coefficients are not directly useful for correcting the effects of antenna gain loss, which require the individual antenna (inverse) voltage correction factors expressed as the coefficients of a polynomial fit to the voltage gain as a function of zenith distance. That is, the AIPS suite of programs can implement gain corrections of the form

$$V_c = G_0 + G_1 Z + G_2 Z^2 + \dots,$$

where V_c is the voltage gain correction of an antenna-IF, and the G_i are the coefficients of a polynomial series. Z is the zenith angle in degrees: $Z = 90 - E$. The preferred method for

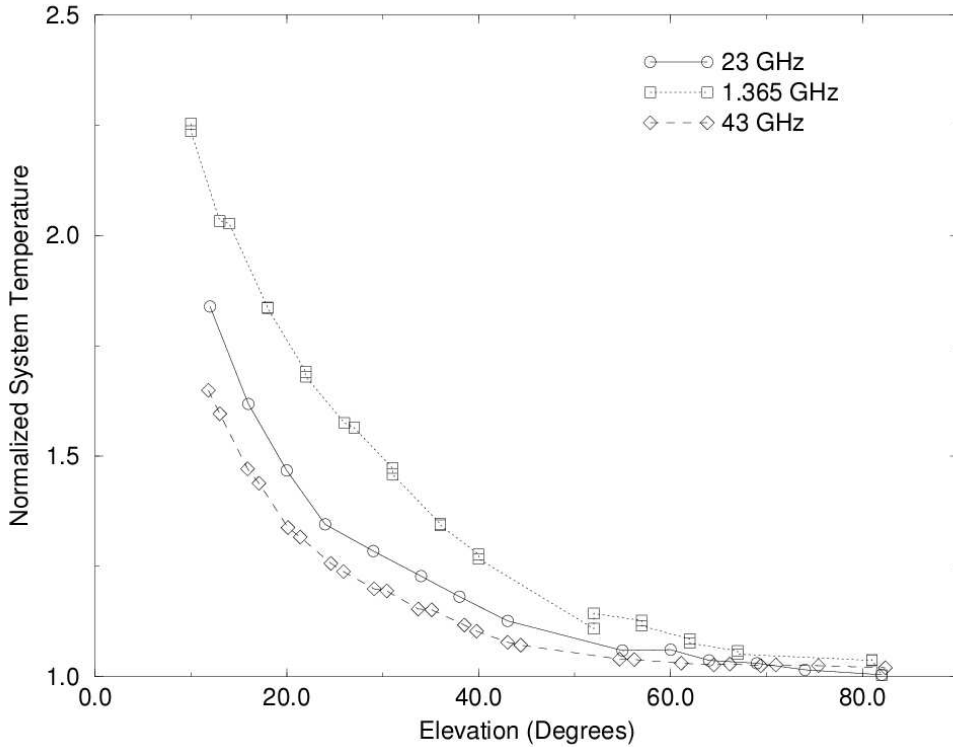


Figure 4: **System Temperature Variations with Elevation at L, K, and Q Bands.** The data have been normalized by the system temperature at the zenith – approximately 80K at 43 GHz, 170K at 23 GHz, and 35K at 1365 MHz. The observations were taken in good weather conditions. Since production of the data for this figure, the VLA 22 GHz receivers were replaced by receivers with much-improved low-noise amplifiers, dramatically reducing the overall system temperature (see Table 3), thus raising the fractional variation at low elevations.

determining these is through direct measurement of the relative system gain using the AIPS task ELINT on data from a strong calibrator which has been observed over a wide range of elevation.

Starting with the 31DEC01 AIPS, the task FILLM applies standard gains and an estimated opacity in CL table version 1. (This correction can be turned off with appropriate parameter choices.) For those with older versions of AIPS or less recent observations, an approximate correction can be obtained using the amplitude coefficients given below in Table 7. These are applied using the AIPS task CLCOR.

Table 7: **Average Inverse Voltage Gain Coefficients for the VLA Antennas**

| Band | G_0 | G_1 | G_2 |
|------|-------|------------------------|-----------------------|
| Q | 1.00 | -1.29×10^{-2} | 1.59×10^{-4} |
| K | 1.00 | -0.41×10^{-2} | 0.69×10^{-4} |
| U | 1.00 | -0.17×10^{-2} | 0.19×10^{-4} |
| X | 1.00 | -0.23×10^{-3} | 0.33×10^{-5} |

These coefficients are averages over all the antennas, and are appropriate for an atmosphere of zero opacity. Considerable differences exist between antennas, particularly for antennas #1 and #2.

When using these coefficients, one must first correct for the opacity (typically measured using the TIPPER procedure), via the AIPS program CLCOR, then apply the gain coefficients in a

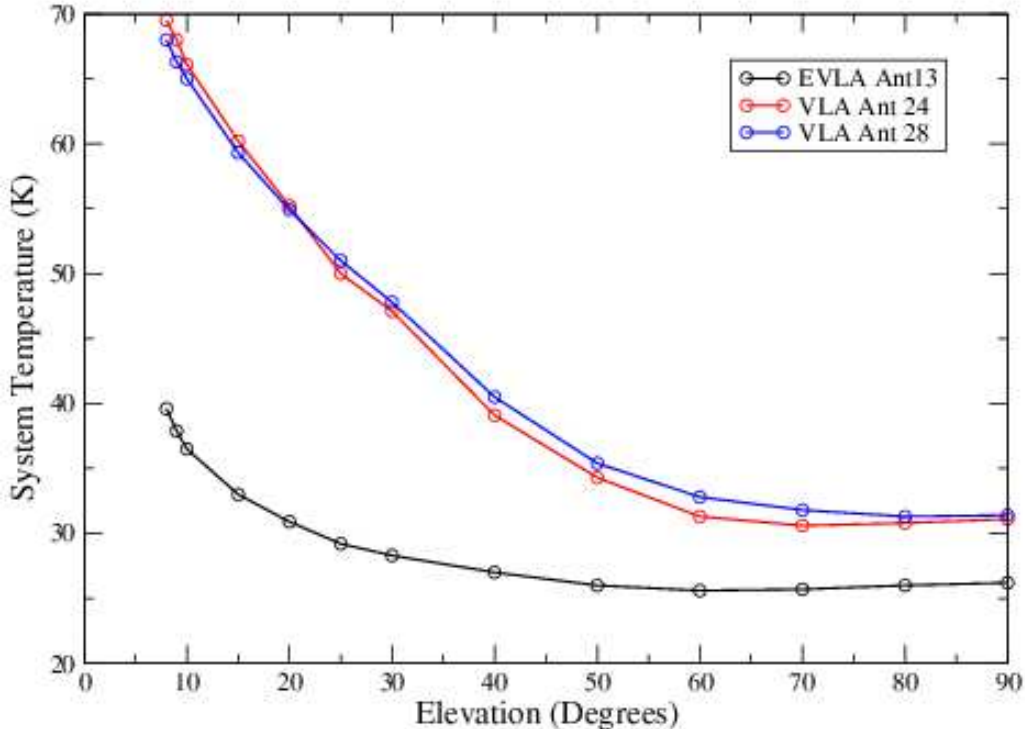


Figure 5: **EVLA System Temperature Variation with Elevation at L Band.** This plot displays the EVLA improvement in system temperature performance as a function of elevation at 1425 MHz. The blue and red lines are standard VLA antennas, while the more shallowly sloped black line is an EVLA antenna. For more details, see EVLA Memo No. 85, available on the web (see Section 6).

subsequent run of CLCOR. The TIPPER procedure is an observing mode on the VLA which entails a simple measurement of the sky brightness as a function of elevation. The on-line software uses these data to derive the atmospheric zenith opacity and system temperature. This observing mode is known to the `JObserve` program. If no measurements were taken, it also is possible to derive an estimate of the opacity from seasonal averages or nearby observations (see <http://www.vla.nrao.edu/astro/calib/tipper/>). Contact Bryan Butler, Steve Myers, or Claire Chandler for advice on these techniques.

3.5 Field of View

At least four different effects will limit the field of view. These are: primary beam; chromatic aberration; time-averaging; and non-coplanar baselines. We discuss each briefly:

3.5.1 Primary Beam

The ultimate factor limiting the field of view is the diffraction-limited response of the individual antennas. An approximate formula for the full width at half power in arcminutes is: $\theta_{\text{PB}} = 45/\nu_{\text{GHz}}$. More precise measurements of the primary beam shape have been derived and are incorporated in the AIPS task PBCOR to allow for correction of the primary beam attenuation in wide-field images. Objects larger than approximately half this angle cannot be directly observed by the array. However, a technique known as ‘mosaicing’, in which many different pointings are taken, can be used to construct images of larger fields. Refer to References 1 and 2 for details, or contact Debra Shepherd.

3.5.2 Chromatic Aberration (Bandwidth Smearing)

The principles upon which synthesis imaging are based are strictly valid only for monochromatic radiation. When radiation from a finite bandwidth is accepted and gridded as if monochromatic, aberrations in the image will result. These take the form of radial smearing which worsens with increased distance from the delay-tracking center. The peak response to a point source simultaneously declines in a way that keeps the integrated flux density constant. The net effect is a radial degradation in the resolution and sensitivity of the array.

These effects can be parameterized by the product of the fractional bandwidth ($\Delta\nu/\nu_0$) with the source offset in synthesized beamwidths ($\theta/\theta_{\text{HPBW}}$). Table 8 shows the decrease in peak response and the increase in apparent radial width as a function of this parameter.

Table 8: Reduction in Peak Response Due to Bandwidth Smearing

| $\frac{\Delta\nu}{\nu_0} \frac{\theta_0}{\theta_{\text{HPBW}}}$ | Peak | Width |
|---|------|-------|
| 0.0 | 1.00 | 1.00 |
| 0.50 | 0.95 | 1.05 |
| 0.75 | 0.90 | 1.11 |
| 1.0 | 0.80 | 1.25 |
| 2.0 | 0.50 | 2.00 |

Note: The reduction in peak response and increase in width of an object due to bandwidth smearing (chromatic aberration). $\Delta\nu/\nu_0$ is the fractional bandwidth; $\theta_0/\theta_{\text{HPBW}}$ is the source offset from the phase tracking center in units of the synthesized beam.

If you wish to obtain maximum sensitivity and resolution over the entire field-of-view of the antennas, then the spectral-line modes of the correlator (also known as multichannel continuum or pseudo-continuum) probably will be required.

3.5.3 Time-Averaging Loss

The sampled coherence function (visibility) for objects not located at the phase-tracking center is slowly time-variable due to the changing array geometry, so that averaging the samples in time will cause a loss of amplitude. Unlike the bandwidth loss effect described above, the losses due to time averaging cannot be simply parameterized. The only simple case exists for observations at $\delta = 90^\circ$, where the effects are identical to the bandwidth effect except they operate in the azimuthal, rather than the radial, direction. The functional dependence is the same in this case with $\Delta\nu/\nu_0$ replaced by $\omega_e \Delta t_{\text{int}}$, where ω_e is the Earth's angular rotation rate, and Δt_{int} is the averaging interval.

For other declinations, the effects are more complicated and approximate methods of analysis must be employed. Chapter 13 of Reference 1 considers the average reduction in image amplitude due to finite time averaging. The results are summarized in Table 9, showing the time averaging in seconds which results in 1%, 5% and 10% loss in the amplitude of a point source located at the first null of the primary beam. These results can be extended to objects at other distances from the phase tracking center by noting that the loss in amplitude scales with $(\theta \Delta t_{\text{int}})^2$, where θ is the distance from the phase center and Δt_{int} is the averaging time. Since the size of VLA continuum data sets typically is not a limiting factor for modern computers, we recommend that most observers reduce the effect of time-average smearing by using integration times of $3\frac{1}{3}$ seconds (also see Section 3.6) in at least the **A** and **B** configurations.

3.5.4 Non-Coplanar Baselines

The procedures by which nearly all images are made in Fourier synthesis imaging are based on the assumption that all the coherence measurements are made in a plane. This is strictly true for E-W interferometers, but is false for the VLA, with the single exception of snapshots. Analysis of the problem shows that the errors associated with the assumption of a planar array increase

Table 9: Loss vs. Averaging Time for Time Averaging Smearing

| Configuration | Amplitude loss | | |
|---------------|----------------|-------|-------|
| | 1.0% | 5.0% | 10.0% |
| A | 2.1 | 4.8 | 6.7 |
| B | 6.8 | 15.0 | 21.0 |
| C | 21.0 | 48.0 | 67.0 |
| D | 68.0 | 150.0 | 210.0 |

Note: The averaging time (in seconds) resulting in the listed amplitude losses for a point source at the antenna first null. Multiply the tabulated averaging times by 2.4 to get the amplitude loss at the half-power point of the primary beam. Divide the tabulated values by 4 if interested in the amplitude loss on the longest baselines.

quadratically with angle from the phase-tracking center. Serious errors result if the product of the angular offset in radians times the angular offset in synthesized beams exceeds unity. The effects are especially severe at the 90 cm and 400 cm bands, where standard two-dimensional imaging can be done only for **D**-configuration data. This effect is noticeable at $\lambda 20$ cm in certain instances, but can be safely ignored at shorter wavelengths.

A solution to the problem of imaging wide-field data taken with non-coplanar arrays is well known, and has been implemented in the AIPS program **IMAGR**. This program can now correctly image up to 512 subfields, sufficient to handle observations in the **B**, **C**, and **D** configurations. We expect that as computer performance continues to improve, full imaging of even **A** configuration data will soon be practical. Refer to the help file for this program, or consult with Rick Perley or Frazer Owen, for advice. More computationally efficient imaging with non-coplanar baselines is being investigated, such as the “W-projection” method; see EVLA Memo 67 for more details.

3.6 Time Resolution

The minimum integration time at which all data can be written to tape is a function of the total number of channels of data produced by the correlator. This minimum time varies from $1\frac{2}{3}$ seconds for the continuum mode to 20 seconds for 512 channel spectral line modes. Note that in order to ensure the complete removal of correlator offsets, averaging times should be an integer multiple of $3\frac{1}{3}$ seconds (which is the period of the Walsh functions that are used to negate cross-coupling between antenna signal lines).

Averaging times shorter than those listed above can be selected, but only at the cost of removing antennas from the array. For the spectral line modes, the approximate relation is that the minimum integration time in seconds equals the total number of baselines plus antennas ($= N(N + 1)/2$) multiplied by the total number of correlated channels (less than or equal to 512) divided by 10,000. In continuum mode, integration times as short as 0.4 seconds are available, but are appropriate only for EVLA/VLA testing and for fast flaring activity such as solar flares. Contact Ken Sowinski for details on their use.

Users should keep in mind the data rate of the VLA when planning their observing. The array’s maximum data rate of more than 3 GByte per day presently is only a minimal problem for the modern computers that most astronomers use for their data reduction. If necessary, this rate may be reduced by increasing the averaging time and/or decreasing the number of spectral channels. Consult one of the spectral line experts listed in Table 16 for advice.

The maximum recommended integration time for any VLA observing is 60 seconds. The maximum allowable integration time in the spectral line modes is 90 seconds. There is no formal limit in the continuum modes, but it is generally reasonable to use the default of 10 seconds. For high frequency observers with short scans (e.g., fast switching, as described in Section 3.13.2), a $3\frac{1}{3}$ second integration time may be preferable.

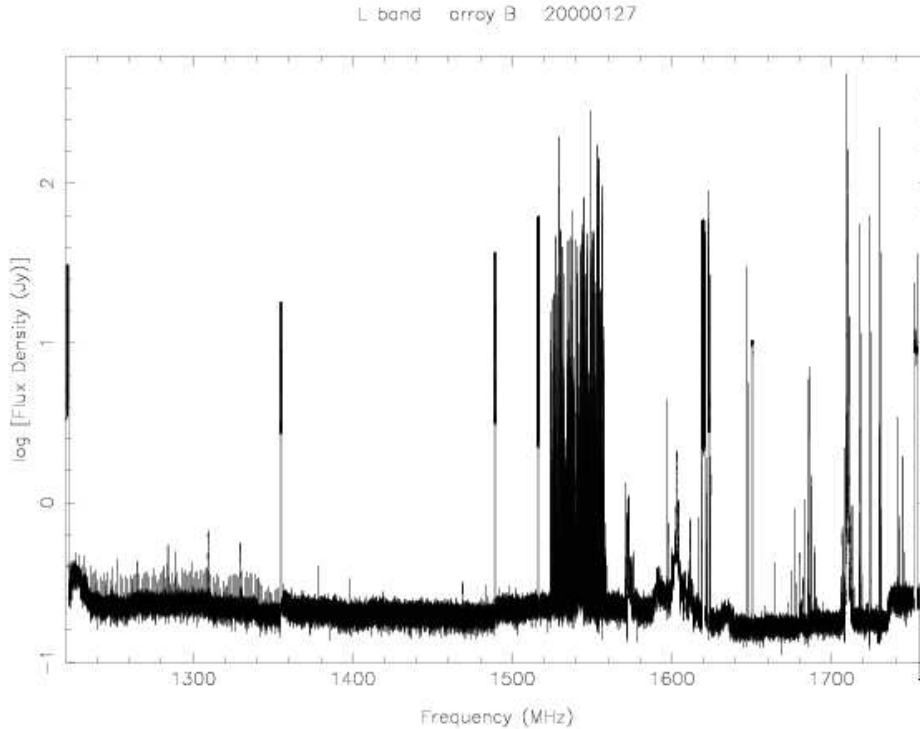


Figure 6: Typical L-band interference Spectrum.

3.7 Radio-Frequency Interference

The bands within the tuning range of the VLA which are allocated exclusively to radio astronomy are 1400 – 1427 MHz, 1660 – 1670 MHz, 4990 – 5000 MHz, 15.35 – 15.4 GHz, 22.2 – 22.5 GHz, and 23.6 – 24.0 GHz. No external interference should occur within these bands. Experience shows that RFI is a serious problem only within the 20, 90, and 400 cm bands. At 20 cm, interference is most serious to the **D** configuration, as the fringe rates in other configurations are often sufficient to reduce interference to tolerable levels.

RFI at the VLA is an increasing problem to astronomical observations. To monitor this increase, and to provide a rough guide to the severity of this interference, the RFI spectrum at all bands from P through K is measured on an occasional basis, using the VLA correlator system. Plots of typical spectra in the L and P bands, taken with 6 kHz resolution, are shown in Figures 6 and 7.

Downloadable plots of all RFI observations from 1993 onwards are available on the Web. For general information about the RFI environment, contact the head of the IPG (Interference Protection Group) by sending e-mail to NRAO-RFI@nrao.edu.

Table 10 is a convenient summary of eight such observations taken during 2001. This table lists the ‘line’ frequency, the average equivalent flux density (in mJy) in 50 MHz, and the peak flux density, also reduced to 50 MHz equivalent bandwidth. A significant difference between these columns indicates that the RFI is intermittent. These equivalent flux densities are approximate, and should be used only to give a rough approximation to the severity and likelihood of a problem. A more detailed version of Table 10 is available on the web at <http://www.vla.nrao.edu/astro/rfi/rfifreqs.txt>.

Between 1220 and 1255 MHz, very strong and very broad RFI is always present, primarily due to the GPS-L2 signal at 1227.6 ± 10 MHz, and a border radar at 1252 ± 1.25 MHz near Deming, New Mexico. It may be possible to observe in selected, narrow bandwidths in this region. Numerous other strong radars belonging to the FAA’s Air Route Surveillance system exist between 1250 and 1350 MHz in the general vicinity of the VLA. Between 1435 and 1530 MHz, aeronautical telemetry from White Sands Missile Range (WSMR) occasionally will interfere with observing. These transmissions

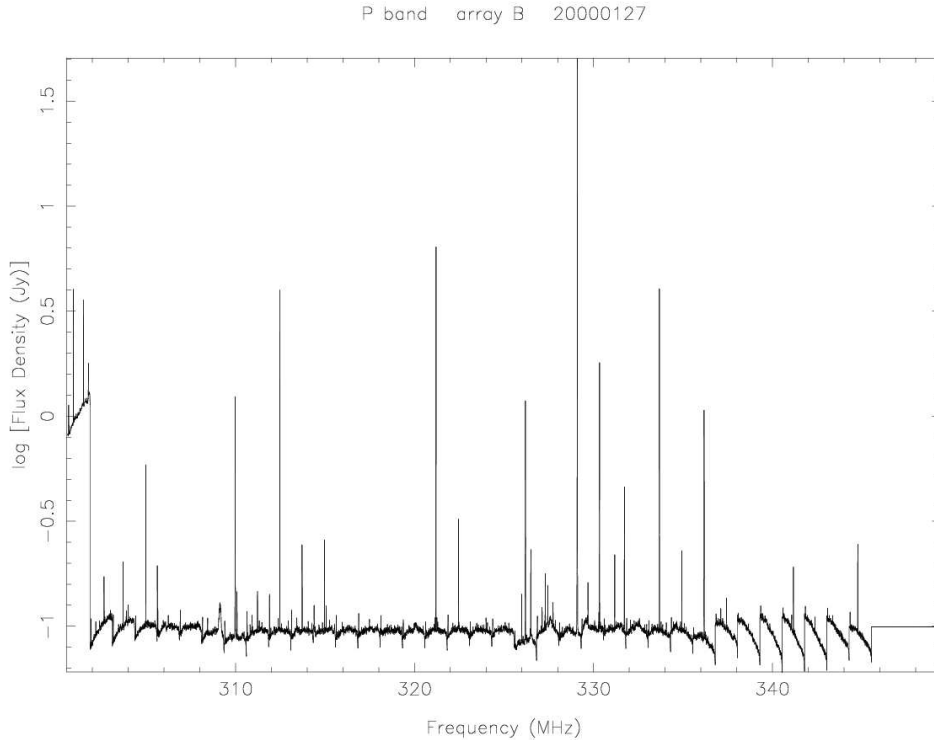


Figure 7: **Typical P-band Interference Spectrum.**

are very occasional, and unpredictable. They are worst in the spring, during the WSMR wargames exercises.

Note that the listed RFI signal strengths are appropriate for the **D** configuration. These signal strengths are considerably reduced in the larger configurations – an average attenuation of perhaps a factor of 100 will be obtained in the **A** configuration due to fringe phase winding.

In late 1998, the Iridium constellation of Low Earth Orbit (LEO) satellites was activated. As is well known, this venture was not a commercial success, but it was purchased by a consortium of investors called Iridium LLC, and is being operated by Boeing. Thus these satellites are still broadcasting in the 1621–1627 MHz band, but their signals are strong enough that VLA observations between 1610 and ~1645 MHz generally are not possible. Filters have been installed to allow 1612 MHz OH observations (see <http://www.vla.nrao.edu/astro/guides/ifilt/>).

In general, it may be possible to observe in spectral regions containing strong RFI provided: (1) That the RFI is not so strong as to cause serious gain compression in the amplifiers, and (2) That the RFI is kept out of the correlator through use of a narrow back-end filter. This latter requirement is particularly important for spectral line correlator modes, although use of Hanning smoothing is very effective in reducing the Gibbs ringing (described in the VLA Spectral Line Users Guide, at <http://www.vla.nrao.edu/astro/guides/sline/current/>). Gain compression in the antenna electronics often can be prevented by using a narrower (12.5 or 25 MHz) “front-end” filter (actually present in the IF stage), rather than the default 50 MHz filter. Note that use of these FE filters greatly restricts the range of tunable frequencies. The scheduling program `JObserve` is aware of these restrictions, and should be used when contemplating use of the narrow front-end filters.

Observers can use Table 10 to assist in deciding which center frequencies and bandwidths are most likely to result in good data at L band. There are very few good combinations for 50 and 25 MHz bandwidths. These are summarized in Table 11, which shows the ‘statistically’ best frequencies to use at L-band with the listed bandwidths. Note that the VLA LO system restricts the selection of frequencies at both 50 MHz and 25 MHz bandwidths. The restrictions are particularly severe

Table 10: **VLA RFI Between 1260 and 1740 MHz**

| Frequency | Avg. Flux | Pk. Flux | Source | Comments |
|-----------|-----------|----------|------------------------|-------------------------|
| 1277 MHz | 12 mJy | 20 mJy | Aerostat Radar | Sometimes absent |
| 1286 | 2 | 5 | Farmington Radar | Other weak lines nearby |
| 1300 | 2 | 5 | Internal RFI | |
| 1310 | 100 | 100 | ABQ Radar | |
| 1316 | ??? | ??? | ABQ Radar | Weaker, often absent |
| 1330 | 45 | 80 | ABQ Radar | Sometimes absent |
| 1381 | 3 | 100 | GPS L3 IONDS | On < 3% of the time |
| 1400 | 60 | 60 | Internal RFI | |
| 1429-1435 | 15 | 130 | Military | Four separate lines |
| 1444,1453 | 5 | > 100 | High Altitude Balloons | NASA/NSBF |
| 1500 | 2 | 5 | Internal RFI | |
| 1515 | 15 | > 100 | High Altitude Balloons | |
| 1525 | 6 | > 100 | High Altitude Balloons | |
| 1530-1544 | > 130 | > 200 | INMARSAT | Many 'lines' |
| 1557-1567 | 10 | 20 | GPS Sidelobe? | Wide spectrum |
| 1570-1580 | > 500 | > 500 | GPS-L2 | Wide spectrum |
| 1600 | 120 | 120 | Internal RFI | |
| 1602-1616 | > 500 | > 500 | GLONASS | Many separate 'lines' |
| 1610-1645 | >500 | >500 | IRIDIUM! | See text |
| 1620 | 80 | 300 | ? | |
| 1650 | 13 | 25 | Internal RFI | |
| 1678-1698 | 50 | 100 | Radiosondes, satellite | > 6 variable 'lines'. |
| 1710 | 10 | 10 | ? | |
| 1714 | > 500 | > 500 | Forest Service | |
| 1725 | 10 | 10 | Forest Service | |
| 1730 | 25 | 25 | Forest Service | |
| 1735 | > 100 | > 100 | Forest Service | |

at a bandwidth of 50 MHz – for a given IF, the only center frequencies (in MHz) which can be observed with that bandwidth are those ending in 15, 35, 65, or 85. (For example, between 1400 and 1500 MHz, the only permitted frequencies are 1415, 1435, 1465 and 1485 MHz.) With the 25 MHz front-end bandwidth filters, regions 5 MHz wide centered on 1250, 1300, 1350, ..., cannot be tuned. And when using the 12 MHz front-end bandwidth filters, 8 MHz wide regions centered at 1225, 1275, 1325, 1375, ..., and 18 MHz wide regions centered at 1250, 1300, 1350, 1400, ..., cannot be reached.

Table 11: **Recommended Center Frequency/Bandwidth Combinations for L Band**

| BW | Class A | Class B | Class C |
|--------|--------------------------|---------------------|-----------------|
| | No RFI Expected | Weak/Occas'l RFI | 'Tolerable' RFI |
| 50 MHz | none | 1365,1435,1465,1485 | 1335,1385,1415 |
| 25 MHz | 1343 – 1347 | 1290 – 1297 | Use Table 10 |
| | 1353 – 1387 ¹ | 1453 – 1470 | |
| | 1413 – 1417 | 1503 – 1517 | |
| | 1663 – 1665 | | |

Footnotes:

1. The White Sands Missile Range uses 1357±3 MHz for airborne telemetry once or twice per week.

The ubiquity of L-band interference makes it difficult for users wishing high sensitivity to find significant bandwidths free of RFI. As a result of monitoring the RFI, we have established a number of standard bands which are more likely to be free of significant RFI. These are shown below in Table 12.

Table 12: JObserve Names of L-band ‘Standard Frequencies’

| JObserve Name | AC | | BD | |
|-----------------|------------------|-----------|------------------|-----------|
| | Center Frequency | Bandwidth | Center Frequency | Bandwidth |
| LL | 1464.9 | 50 | 1385.1 | 50 |
| L1 ¹ | 1364.9 | 50 | 1435.1 | 50 |
| L2 | 1515.9 | 25 | 1365.1 | 25 |
| L3 | 1515.9 | 25 | 1435.1 | 25 |

Footnotes:

1. The L1 frequency combination was used for the NVSS and FIRST surveys.

Another important form of RFI consists of signals which are generated by each antenna. These signals are picked up by nearby antennas, or by the generating antenna’s feed, and produce correlated signals in the visibility data. This form of RFI is especially important in the P and 4 bands when in the **C** and **D** configurations. They appear at all multiples of 5 and 12.5 MHz - frequencies divisible by these numbers must be avoided. (It is this spectrum of RFI which limits our P-band bandwidth to 3.125 MHz.) Another family of RFI occurs at multiples of 100 kHz - these are much weaker and can be ignored for continuum work at 90 cm, but are important on many baselines at the 400 cm band.

At P band, the RFI situation can be particularly difficult. Interference is relatively infrequent in the evenings and on weekends, but during the day, very strong interference – sufficient to saturate the receivers – is common. The best advice is to arrange observing to fall outside of regular working hours. Very sensitive spectral line observations at P band require special measures at the VLA site to turn off known sources of RFI. To implement these measures, contact the interference protection group (see Table 16). The situation at 4 band generally is better, as nearly all of the RFI is weak and is generated by the antennas themselves (see above); the self-generated RFI can be removed in processing provided the spectral line correlator mode is employed.

At P and 4 bands, use of the spectral line correlator modes is strongly recommended for all observations to allow diagnosis and removal of internal and external interference. For observations which do not require linear polarization information, use of the correlator modes ‘1x’, ‘2xy’, or ‘4’ is recommended to maximize the spectral resolution. The labels ‘x’ and ‘y’ are the IF designators, A, B, C, or D. Refer to Section 2 for a description. The current default for 327 MHz is now ‘4’.

For L, C, K, and Q bands, observers should avoid using an L6 (second LO) setting of 3760 or 3790 MHz, due to an internal birdie produced by those LO settings. For X and U bands, avoid using 3840 and 3810 MHz. The JObserve program is aware of these restrictions, so users should not inadvertently fall victim to this problem.

3.8 Antenna Pointing

The pointing parameters of the antennas are measured monthly under calm nighttime conditions. The antenna model, using these parameters, suffices under good weather to allow blind pointing to an accuracy of about 10 arcsec rms. The pointing accuracy in daytime is a little worse, due to the effects of solar heating of the antenna structures.

Moderate winds have a very strong effect on both pointing and antenna figure. The advertised maximum wind speed for precision operations is 15 mph (7 m/s), and careful observations have demonstrated this to be the practical maximum wind speed for useful observing at K and Q bands. Observations at these bands in winds significantly in excess of this limit are not advisable, and users should consider moving to a lower frequency. Wind speeds near the stow limit (45 mph) will have a similar negative effect at X and U bands.

To achieve better pointing, we have added a capability for repeated calibration and correction of the local pointing error during astronomical observations. In this observing mode, known as ‘referenced pointing’, a nearby calibrator is observed in interferometer pointing mode every hour or so. The local pointing corrections thus measured can then be applied to subsequent target observations. Tests show that this mode reduces rms pointing errors to typically 2 – 3 arcseconds if the reference source is within about 10 degrees (in azimuth and elevation) of the target source, and the source elevation is less than 70 degrees. The `JObserve` program is aware of this observing mode.

Use of referenced pointing is highly recommended for all K- and Q-band observations, and for X- and U-band observations of objects whose total extent is a significant fraction of the antenna primary beam. It is usually recommended that the referenced pointing measurement be made at X-band, regardless of what band your target observing is at, since X-band is the most sensitive, and the closest calibrator is likely to be rather weak. Proximity of the reference calibrator to the source position is of paramount importance. The calibrator should have at least 300 mJy flux density and be unresolved on all baselines to ensure an accurate solution.

Measuring the pointing offsets at K-band for subsequent K-band observing is usually successful, but should not be attempted on objects of less than 300 mJy flux density. However, attempting to measure these offsets at Q-band directly generally is not recommended, since the blind pointing error is often larger than the Q-band half-power half-width – which will cause the referenced pointing to fail.

Secondary referenced pointing (*i.e.*, using X-band referenced pointing to permit subsequent Q-band or K-band determination of the residual pointing errors), is recommended only for high precision observations at Q and K bands when observing extended objects which fill the antenna primary beam. For general observing of small objects, simple referenced pointing using the offsets determined at X-band is nearly always sufficient to keep all antennas pointing to within 5 arcseconds.

Consult with Rick Perley, Ken Sowiński, or Claire Chandler for more information about referenced pointing. The information above is largely taken from the guide to high-frequency observing on the VLA, found at <http://www.vla.nrao.edu/astro/guides/highfreq/>.

3.9 Subarrays

The VLA can simultaneously process five different observing programs. However, the subarrays are not all fully independent. If use of this capacity is contemplated, the following limitations must be understood and followed:

1. Each subarray uses a different observing file. (Strictly speaking, this is not a requirement, but is sensible.) The VLA operator must be told which file is to control which subarray, and which antennas are to be in each subarray. Antenna ‘shuffling’, in which antennas are reassigned from one subarray to another after observing has begun, is **strongly discouraged**.
2. Only one integration time for the entire array can be defined. Unless told otherwise, this time is that assigned for subarray #1. All other requested integration times (which are given on the `//DS` card in the observing control file) are ignored.
3. All subarrays must be in continuum mode, or all must be in spectral line mode. Any spectral line/continuum mix will result in **no data** at all. This is true for both standard observing and for a pointing determination.
4. If an IF (*i.e.* A, B, C, or D) is used in more than one subarray, it must have the same bandwidth in each. (This restriction applies only to spectral line observations).
5. There are only two sets of Fluke synthesizers (the final LOs in the frequency conversion system) – hence, only two subarrays can have completely independent frequency selection. If using two subarrays, notify the operator about your requirements for synthesizer setting – this selection is not made within the observing file. For three or more subarrays, a decision will have to be made on which subarrays will be ‘slaved’. This will constrain the frequencies used for bandwidths other than 50 MHz.

Note that tipping scans (used to measure the atmospheric opacity) can be done at any time by any number of subarrays. If any of the above restrictions confuse you (and we are sympathetic if they do), consult a VLA staff member, or talk to Ken Sowiński.

Single-antenna (or multiple-antenna) VLBI programs cause special problems. Such programs use one of the Fluke sets, leaving only one for the remaining four subarrays – these must then share that single Fluke set, or use the same values assigned to the VLBI run. Generally, VLBI Fluke settings are compatible with continuum observing. Fortunately, the correlator restrictions listed above (points 3 and 4) do NOT apply to the single-antenna VLBI subarrays.

3.10 Positional Accuracy

The accuracy with which an object’s position can be determined is limited by the atmospheric phase stability, the closeness of a suitable (astrometric) calibrator, and the calibrator-source cycle time. Under good conditions, in **A** configuration, accuracies of about 0.05 arcseconds can be obtained. Under more normal conditions, accuracies of perhaps 0.1 arcseconds can be expected. Under extraordinary conditions (probably attained only a few times per year on calm winter nights in **A** configuration when using rapid phase switching on a nearby astrometric calibrator – see Section 3.13.2), accuracies of 1 milliarcsecond have been attained.

If highly accurate positions are desired, only ‘A’ code (astrometric) calibrators from the VLA Calibrator List should be used. The positions of these sources are taken from lists published by the USNO.

3.11 Limitations on Imaging Performance

Imaging performance can be limited in many different ways. Some of the most common are listed in the following subsections.

3.11.1 Image Fidelity

With conventional point-source calibration methods, and even under the best observing conditions, the achieved dynamic range will rarely exceed a few hundred. The limiting factor is the atmospheric phase stability. If the target source contains more than 50 mJy⁵ in compact structures (depending somewhat on band), self-calibration can be counted on in improving the images. Dynamic ranges in the thousands can be achieved using these techniques. At this level, the limitations are generally due to errors in the calculation of the correlation coefficient (‘closure’ errors). Recent (1998) software changes in the VLA’s calculation of these coefficients have dramatically reduced the level of these errors for VLA-only continuum observing, particularly for the narrower bandwidths where these errors were larger.

If the target source is bright enough for dynamic ranges exceeding 10,000 (based on peak/rms thermal noise) to be conceivable, use of one of the spectral line correlator modes should be considered, since the correlator errors which limit the dynamic range are greatly reduced. However, due to inherent limitations in correlator capacity, this will necessarily require a reduction in bandwidth by a factor of at least four. If the target source is only slightly resolved, use of the continuum mode with phased array observing will reduce the ‘closure’ errors without loss of bandwidth.

3.11.2 VLA-EVLA Closure Errors

Antenna calibration algorithms generally assume that calibration quantities (both in the antennas and in the atmosphere) can be separated on an antenna-by-antenna basis. This provides substantial strength in determining calibration quantities, since (for 27 antennas) 351 baselines of interferometer visibility data may be used to determine 27 individual calibration values, one for each antenna. However, this assumption breaks down for a mixed array of VLA antennas and retrofitted EVLA antennas, since the improved EVLA bandpass response functions are not matched exactly to the

⁵This limiting successful flux density can be considerably lower, if the atmospheric coherence time is many minutes, or higher, for short coherence times and noisier frequencies

poorer (but identical to each other) bandpass responses of VLA antennas. A symptom of the breakdown of this assumption is excessive amplitude closure errors when running the AIPS task **CALIB**, where the EVLA-EVLA baselines may be reported to have closure errors as high as 3% to 8% for 50 MHz bandpasses, or even larger for narrower bandpasses. The closure errors originate in the mismatch of the VLA-EVLA bandpasses and the **CALIB** assumption that all calibration quantities are antenna-based, rather than in any EVLA characteristic, but the ultimate result is a miscalibration of the EVLA-EVLA baselines.⁶ For continuum observations, the closure errors may be calibrated by observing a strong calibrator and solving for baseline-dependent errors using the AIPS task **BLCAL**. For spectral-line observations, the standard bandpass calibrations (e.g., AIPS task **BPASS**) also will remove the effects of the mismatched bandpasses.

3.11.3 Invisible Structures

An interferometric array acts as a spatial filter, so that for any given configuration, structures on a scale larger than the fringe spacing of the shortest baseline will be completely absent. Diagnostics of this effect include dark bowls around extended objects, and large-scale stripes in the image. Table 2 gives the largest scale visible to each configuration/band combination.

3.11.4 Poorly Sampled Fourier Plane

Unmeasured Fourier components are assigned values by the deconvolution algorithm. While this often works well, sometimes it fails noticeably. The symptoms depend upon the actual deconvolution algorithm used. For the **CLEAN** algorithm, the tell-tale sign is a fine mottling on the scale of the synthesized beam, which sometimes even organizes itself into coherent stripes. Further details are to be found in Reference 1.

3.11.5 Sidelobes from Confusing Sources

At 90 and 20 cm, large numbers of background sources are located throughout the primary antenna beam. Sidelobes from these objects will lower the image quality of the target source. Although bandwidth and time-averaging will tend to reduce the effects of these sources, the very best images will require careful imaging of all significant background sources. The AIPS task **IMAGR** is well suited to this task at 20 cm. The problem at 90 cm is much worse, and is greatly complicated by the non-coplanar nature of the array, as described in Section 3.5.4. Table 2 gives the highest flux density expected of these background sources, and the total background flux density. Note that there is an NVSS RUN file generator (available from the NVSS page at <http://www.cv.nrao.edu/nvss/>) that can be extremely helpful in defining the fields containing confusing sources.

3.11.6 Sidelobes from Strong Sources

Another image-degrading effect is that due to strong nearby sources. Again, the 20 and 90 cm bands are especially affected. The active Sun will be visible to any **D** configuration daytime spectral line observation at these bands. Even with 50 MHz bandwidth in continuum mode, the active Sun can ruin the short spacings of observations within about 20 degrees of the Sun. The quiet Sun poses a lesser threat, so the general rule is to go ahead and observe, even if the target source is close to the Sun. At 90 and 400 cm, observations within approximately 10 degrees of Cygnus A, Cassiopeia A, Taurus A, and Virgo A will be greatly degraded.

3.12 Calibration and the Flux Density Scale

The VLA Calibrator List contains information on 1860 sources sufficiently unresolved and bright to permit their use as calibrators. Copies of the list are distributed throughout the AOC. The list is

⁶When equal numbers of VLA and EVLA antennas are in the operational array, expected in late 2007 or early 2008, the positive closure errors on EVLA-EVLA baselines will be about equal in magnitude to the negative closure errors reported for VLA-VLA baselines.

also available within the JObserve program and may be accessed on the Web at <http://www.vla.nrao.edu/astro/calib/manual/>.

Accurate flux densities can be obtained by observing one of 3C286, 3C147, 3C48 or 3C138 during the observing run. Not all of these are suitable for every observing band and configuration – consult the VLA Calibrator Manual for advice. Over the last several years, we have implemented accurate source models directly in AIPS for much improved calibration of the amplitude scales; see page 21 of the July 2006 NRAO Newsletter for details. At present, models are available for 3C48 and 3C286 for all bands from 1.3 to 20 cm, for 3C138 at all bands from 1.3 to 6 cm, and for 3C147 at all bands from 0.7 to 2.0 cm.

Since the standard source flux densities are slowly variable, we monitor and update their flux densities when the VLA is in its **D** configuration. As the VLA cannot measure *absolute* flux densities, the values obtained must be referenced to assumed or calculated standards, as described in the next paragraph. Table 13 shows the flux densities of these sources in November 2001 at our standard bands. The accuracy of these values, relative to the assumed standards, is set by the gain stability of the VLA. The estimated 1- σ errors in the table, relative to the assumed standards, are less than 1% for frequencies up to 25 GHz, and about 2% for the 43 GHz band.

The flux densities shown in the table for frequencies below 10 GHz are based on the Baars *et al.* value for 3C295. For frequencies above 10 GHz, the flux densities are based on models of Mars and NGC 7027 which are themselves based on the Baars scale below 10 GHz.

Polynomial coefficients describing the derived flux densities for the standard calibrators have been determined which permit accurate interpolation of the flux density at any VLA frequency. These coefficients are updated approximately every few years, and are implemented into the AIPS task SETJY. At present, a substantial new effort is under way to improve the long-term (past and present) accuracy of the VLA flux density scale; contact Rick Perley or Bryan Butler for information on this work.

Table 13: Flux densities (Jy) of Standard Calibrators for November 2001

| Source/Frequency (MHz) | 327.5 | 1465 | 4885 | 8435 | 14965 | 22460 | 43340 |
|------------------------|-------|-------|-------|-------|-------|-------|-------|
| 3C48 = J0137+3309 | 45.52 | 15.54 | 5.47 | 3.22 | 1.83 | 1.23 | 0.63 |
| 3C138 = J0521+1638 | 19.34 | 8.16 | 3.71 | 2.43 | 1.54 | 1.10 | 0.62 |
| 3C147 = J0542+4951 | 55.00 | 21.32 | 7.88 | 4.72 | 2.77 | 1.93 | 1.11 |
| 3C286 = J1331+3030 | 25.96 | 14.49 | 7.49 | 5.22 | 3.51 | 2.63 | 1.58 |
| 3C295 = J1411+5212 | 60.37 | 21.49 | 6.53 | 3.42 | 1.67 | 0.99 | 0.41 |
| NGC7027 | <0.2 | 1.54 | 5.52 | 6.03 | 5.90 | 5.68 | 5.22 |
| MARS | – | – | 0.175 | 0.528 | 1.67 | 3.81 | 14.22 |

For most observing projects, the effects of atmospheric extinction will automatically be accounted for by regular calibration when using a nearby point source whose flux density has been determined by an observation of a flux density standard taken at a similar elevation. However, at high frequencies (most notably K-band and Q-band), both the antenna gain and the atmospheric absorption may be strong enough to make ‘simple’ flux density bootstrapping unreliable. The AIPS task ELINT is now available to permit measurement of an elevation gain curve using your own observations, and subsequent adjustment of the derived gains to remove these elevation-dependent effects. The current calibration methodology does not require knowledge of the atmospheric extinction (since the true flux densities of the standard calibrators are believed known). However, if knowledge of the actual extinction is desired, a simple antenna tipping procedure is available (and is known to the JObserve program) which will provide both the vertical extinction and the total system temperature. For advice on these procedures, contact Bryan Butler, Rick Perley, or Claire Chandler.

3.13 Phase Calibration

3.13.1 General Guidelines for Phase Calibration

Adequate phase calibration is a complicated function of source-calibrator separation, frequency, array scale, and weather. And, since what defines adequate for some experiments is completely inadequate for others, it is impossible to define any simple guidelines to ensure adequate phase calibration in general. However, some general statements remain valid most of the time. These are given below.

- Tropospheric effects dominate at wavelengths shorter than 20 cm, ionospheric effects dominate at wavelengths longer than 20 cm.
- Atmospheric (troposphere and ionosphere) effects are nearly always unimportant in the **C** and **D** configurations at L and P bands, and in the **D** configuration at X and C bands. Hence, for these cases, calibration need only be done to track instrumental changes – once per hour is generally sufficient.
- If your target object has sufficient flux density to permit self-calibration, there is no need to calibrate more than once hourly.
- The smaller the source-calibrator angular separation, the better. In deciding between a nearby ‘S’ calibrator, and a more distant ‘P’ calibrator, the nearby calibrator is usually the better choice.
- At high frequencies, and longer configurations, rapid switching between the source and nearby calibrator is often helpful. See the following section.

3.13.2 Rapid Phase Calibration and the Atmospheric Phase Interferometer (API)

For some objects, and under suitable weather conditions, the phase calibration can be considerably improved by rapidly switching between the source and calibrator. An observing technique denoted ‘fast switching’ has been developed to more conveniently permit the user to implement this methodology. Source-Cal observing cycles as short as 40 seconds can now be used – such a short cycle is impossible with traditional VLA observing techniques.

This method is not for everyone! Considerable integration time is lost with very short cycle times, so it is important to balance this certain loss against a realistic estimate of the possible gain. Experience has shown that cycle times of 100 to 150 seconds at high frequencies have been effective for source-calibrator separations of less than 10 degrees. The fast switching technique ‘stops’ tropospheric phase variations at an effective baseline length of $\sim v_a t/2$ where v_a is the atmospheric wind velocity aloft (typically 10 to 15 m/sec), and t is the total switching time. This technique has been demonstrated to result in images of faint sources with diffraction-limited spatial resolution on the longest VLA baselines. Under average weather conditions, and using a 120 second cycle time, the residual phase at 43 GHz should be reduced to ≤ 30 degrees. Further details can be found in VLA Scientific Memos # 169 and 173. These memos, and other useful information, can be obtained from Reference 12 in Section 6.

The fast switching system has been implemented in the current version of the **JObserve** program. Note that the technique will not work in bad weather (such as rain showers, or when there are well-developed convection cells – most notably, thunderstorms). Contact Claire Chandler or Chris Carilli for details and advice, and see the high-frequency observing guide at <http://www.vla.nrao.edu/astro/guides/highfreq/>.

The NRAO Atmospheric Phase Interferometer (API) is now operational at the VLA, and software has been installed for real time monitoring of the phase stability through the web. A detailed description of the API, and instructions for accessing its data, may be found at <http://www.vla.nrao.edu/astro/guides/api/>. The API continuously measures the tropospheric contribution to the interferometric phase using an interferometer comprised of two 1.5 meter antennas separated by 300 meters, observing an 11.3 GHz beacon from a geostationary satellite. The API

data can be used to estimate the required calibration cycle times when using fast switching phase calibration, and in the worst case, to indicate to the observer that high frequency observing may not be possible with current weather conditions. Contact Chris Carilli for further details.

3.14 Polarization

The continuum correlator mode provides full polarimetric information for both observing frequencies. The polarimetric spectral line modes (PA and PB) are also available for observations of linearly polarized spectral lines, or for observations of continuum objects where large field-of-view or high dynamic range is necessary. Spectral line modes ‘2AC’, ‘2BD’, and ‘4’ do not provide linear polarization information.

For each observation requiring polarization information, the instrumental polarization should be determined through observations of a bright calibrator source spread over a range in parallactic angle. In nearly all cases, the phase calibrator chosen can double as a polarization calibrator. The minimum condition that will enable accurate polarization calibration is four observations of a bright source spanning at least 90 degrees in parallactic angle. The accuracy of polarization calibration is generally better than 0.5% for objects small compared to the antenna beam size. At least one observation of 3C286 or 3C138 is required to fix the absolute position angle of polarized emission. 3C48 also can be used to fix the position angle at wavelengths of 6 cm or shorter. The results of a careful monitoring program of these and other polarization calibrators will be found at <http://www.vla.nrao.edu/astro/calib/polar/>.

High sensitivity linear polarization imaging may be limited by time dependent instrumental polarization, which can add low levels of spurious polarization near features seen in total intensity and can scatter flux throughout the polarization image, potentially limiting the dynamic range. The instrumental polarization averaged among all baselines can vary by 0.3% on timescales of minutes to hours, limiting the believable fractional polarization to about 0.1%.

Wide field linear polarization imaging will be limited by the instrumental polarization beam. For a snapshot observation, the spurious linear polarization (after the standard polarization correction for the on-axis polarization response is applied) is $< 1\%$ at angles less than $\lambda/4D$ radians (D is the antenna diameter), is $1 - 3\%$ at $\lambda/2D$, and increases sharply beyond this, reaching 10% at $3\lambda/4D$. Since the instrumental polarization response is directed radially and rotates with parallactic angle, the spurious polarization will tend to average down for long integrations. However, if the object being observed is very bright, and has a low degree of linear polarization, errors in the polarization calibration will cause Stokes I flux to be scattered into the Q and U images, thus limiting the polarization dynamic range.

Ionospheric Faraday rotation is always present at 20 cm and 90 cm. The typical daily maximum rotation measure under quiet solar conditions is 1 or 2 radians/m², so the ionospherically-induced rotation of the plane of polarization at these bands is not excessive – 5 degrees at 20 cm, and perhaps 90 degrees at 90 cm. However, under active conditions, this rotation can be many times larger, such that accurate polarimetry is impossible at 20 cm.

The AIPS program TECOR has been shown to be quite effective in removing large-scale ionospherically induced Faraday Rotation. It uses currently-available data in IONEX format. Please consult the TECOR help file for detailed information.

Circular polarization measurements are limited by the beam squint – the RCP and LCP primary beams are separated by 6 percent of the beamwidth along the axis perpendicular to the azimuth of the secondary focus feed position. Since circular polarization is determined from the difference between RCP and LCP signals, there results an appreciable error in all measurements of circular polarization off the pointing axis. The effect is large – the apparent circular polarization is $\sim 10\%$ at $\lambda/4D$, and $\sim 20\%$ at $\lambda/2D$. This false circular polarization is antisymmetric with respect to the center of the antenna beam, so 12-hour observations should partially cancel out the effect – however, even so, the residual apparent circular polarization is probably only accurate to a few percent.

Observers should be aware that detailed polarization tests have not yet been carried out for the retrofitted EVLA antennas. In particular, we expect that the VLA-EVLA baselines may have non-closing calibration problems similar to the total-intensity calibration (see Section 3.11). This is

complicated by the fact that some receivers on EVLA antennas will be completely new (e.g., wide band 5 GHz receivers), while others will be older VLA systems (e.g., some 8 GHz receivers).

3.15 Spectral Line Modes

The VLA correlator is very flexible, and can provide data in many ways. The various spectral line modes currently available are shown in Tables 14 and 15 and described below.

Table 14: Available Bandwidths and Numbers of Spectral Line Channels in Normal Mode

| BW Code | Bandwidth MHz | Single IF Mode ¹ | | Two IF Mode ² | | Four IF Mode ³ | |
|---------|---------------|-----------------------------|-----------|----------------------------------|-----------|----------------------------------|-----------|
| | | No. Channels ⁴ | Freq. kHz | No. Channels ⁴ per IF | Freq. kHz | No. Channels ⁴ per IF | Freq. kHz |
| 0 | 50 | 16 | 3125 | 8 | 6250 | 4 | 12500 |
| 1 | 25 | 32 | 781.25 | 16 | 1562.5 | 8 | 3125 |
| 2 | 12.5 | 64 | 195.313 | 32 | 390.625 | 16 | 781.25 |
| 3 | 6.25 | 128 | 48.828 | 64 | 97.656 | 32 | 195.313 |
| 4 | 3.125 | 256 | 12.207 | 128 | 24.414 | 64 | 48.828 |
| 5 | 1.5625 | 512 | 3.052 | 256 | 6.104 | 128 | 12.207 |
| 6 | 0.78125 | 512 | 1.526 | 256 | 3.052 | 128 | 6.104 |
| 8 | 0.1953125 | 256 | 0.763 | 128 | 1.526 | 64 | 3.052 |
| 9 | 0.1953125 | 512 | 0.381 | 256 | 0.763 | 128 | 1.526 |

Footnotes:

1. Observing Modes 1A, 1B, 1C, 1D.
2. Observing Modes 2AB, 2AC, 2AD, 2BC, 2BD, 2CD.
3. Observing Modes 4, PA, PB. Note that modes PA and PB only provide correlations for a single IF pair (A & C for mode PA, or B & D for mode PB). Mode 4 provides correlations from both IF pairs (A & C and B & D), but without any cross hand correlation products. It is possible to use the output from one, two or four IFs in such a way as to obtain different combinations of number of spectral line channels and channel separation. The minimum and maximum number of channels is 4 and 512 respectively.
4. These are the numbers of spectral line channels produced in the array processor. Any number of spectral line channels that is a power of 2, that is less than or equal to the number in the table and that is greater than or equal to 2 may be selected using the data selection options available within the `JObserve` program.

Most spectral line modes are distinguished by a code comprising a number followed by zero, one, or two letters. The number refers to the number of spectra being produced; the letters describe which IF channels are involved. Recall that each VLA antenna returns four signals: these are the RCP and LCP for each of two separately tuned frequencies. These signals are referred to as *IFs*, and are named A, B, C, and D. The first two represent RCP, and latter two LCP. IFs A and C are at one frequency (and cannot be different); B and D are at another (and also must be the same). In normal usage, the AC pair and the BD pair are at different frequencies within the same band. The spectral line modes can subdivide these IFs into 4 to 512 units, evenly spaced in frequency across the bandwidth of the input IF. These narrower units are referred to as *spectral line channels*. In addition to these interferometric spectra, autocorrelation spectra for all antennas are produced.

The single-IF modes provided by the spectral line correlator are known as 1A, 1B, 1C, and 1D. In these modes, only one spectrum is produced. These modes give the highest spectral resolution at any given bandwidth. The dual-IF modes are denoted 2AB, 2AC, 2AD, 2BC, 2BD and 2CD, and provide spectral information for the two IFs named (*e.g.* mode 2AC provides AA and CC correlations). Linear polarization measurements are not possible with these modes, but circular polarization can be determined using the 2AC and 2BD modes. The four-IF modes are known as 4, PA and PB. The first of these provides spectra for all four IFs. Circular, but no linear polarization measurements are possible in this mode. The other two modes provide full polarimetric information – PA provides this for the A and C IFs (that is, it performs the correlations AA, AC, CA, and CC, providing a spectrum for each), PB for the B and D IFs. For the 4IF modes very few channels are available

Table 15: Available Bandwidths and Numbers of Spectral Line Channels in Hanning Smoothing Mode

| BW Code | Bandwidth MHz | Single IF Mode ¹ | | Two IF Mode ² | | Four IF Mode ³ | |
|---------|---------------|-----------------------------|------------------|----------------------------------|------------------|----------------------------------|------------------|
| | | No. Channels ⁴ | Freq. Separ. kHz | No. Channels ⁴ per IF | Freq. Separ. kHz | No. Channels ⁴ per IF | Freq. Separ. kHz |
| 0 | 50 | 8 | 6250 | 4 | 12500 | 2 | 25000 |
| 1 | 25 | 16 | 1562.5 | 8 | 3125 | 4 | 6250 |
| 2 | 12.5 | 32 | 390.625 | 16 | 781.25 | 8 | 1562.5 |
| 3 | 6.25 | 64 | 97.656 | 32 | 195.313 | 16 | 390.625 |
| 4 | 3.125 | 128 | 24.414 | 64 | 48.828 | 32 | 97.656 |
| 5 | 1.5625 | 256 | 6.104 | 128 | 12.207 | 64 | 24.414 |
| 6 | 0.78125 | 256 | 3.052 | 128 | 6.104 | 64 | 12.207 |
| 8 | 0.1953125 | 128 | 1.526 | 64 | 3.052 | 32 | 6.104 |
| 9 | 0.1953125 | 256 | 0.763 | 128 | 1.526 | 64 | 3.052 |

Footnotes:

1. Observing Modes 1A, 1B, 1C, 1D.
2. Observing Modes 2AB, 2AC, 2AD, 2BC, 2BD, 2CD.
3. Observing Modes 4, PA, PB. Note that modes PA and PB only provide correlations for a single IF pair (A & C for mode PA, or B & D for mode PB). Mode 4 provides correlations from both IF pairs (A & C and B & D), but without any cross hand correlation products.
4. These are the numbers of spectral line channels produced in the array processor. Any number of spectral line channels that is a power of 2, that is less than or equal to the number in the table, and that is greater than or equal to 2 may be selected using the data selection parameters available in the `OBSERVE` and `JOBSERVE` programs.

at the widest bandwidths and the bandpass formed has high spectral sidelobes. These sidebands will cause non-closing errors on sources distant from the delay tracking center. It is believed that modes PA and PB with 50 MHz bandwidth are unusable for any practical case. Whether a 25 MHz bandwidth is usable or not depends on the complexity of the field imaged and the required dynamic range. For the polarimetric modes, the descriptor 4 is omitted. The characteristics of all of these modes are summarized in Tables 14 and 15.

It is also possible to use multiple, independent subarrays in spectral line mode.

Correlator modes 2AB, 2AD, 2BC and 4 allow the IFs to use different bandwidths as well as to be tuned to different frequencies within the same band (e.g., mode 2AB will permit the AA correlations to be at a different frequency and bandwidth than the BB correlation). There are other restrictions. See Section 3.9, and the Spectral Line Users' Guide (listed in Chapter 6) for details.

Of central interest to observers is the stability of the spectra. Spectral line dynamic range is commonly defined as the ratio of the peak brightness in the strongest channel to the minimum detectable line brightness in an image. This ratio is limited by instrumental effects which must be calibrated out. The spectral dynamic range depends on bandwidth in a poorly understood way. Applying the on-line autocorrelation bandpass correction only should result in about 50:1 dynamic range and is strongly discouraged. Values exceeding 10,000:1 at C and X-bands can be achieved but require careful data editing and bandpass calibration. A more typical limit is around 1000:1. L-band spectral dynamic ranges of 1000:1 can be achieved by observing a suitable bandpass calibrator. Consult with Michael Rupen or another spectral line expert for more details.

Because the operational array currently consists of a mix of VLA and EVLA antennas, there are a number of additional complexities for spectral line observations, listed below:

Doppler tracking: Because the VLA and EVLA antennas will be controlled by different computers until approximately mid-2007, Doppler shift calculations are implemented differently, and Doppler tracking will not work for the VLA-EVLA baselines. Instead, fixed frequencies should be used.

Closure errors: One may expect significant closure errors on VLA-EVLA baselines due to their

very different bandpasses; see Section 3.11 for more information.

Phase jumps and narrow bandpasses: The fine frequency tuning of the VLA is done by a set of “Fluke” synthesizers that may be set to an accuracy of 1 Hz. However, these synthesizers undergo frequent phase jumps when they are set to an accuracy better than 1 MHz (i.e., when any digits to the right of the decimal point are non-zero), and occasional phase jumps even for settings at integer numbers of megahertz. This has no impact on VLA-VLA baselines, since all antennas jump together. However, the EVLA antennas do not use the Fluke synthesizers, and do not undergo the frequent phase jumps, so VLA-EVLA baselines are compromised. We recommend that observers avoid the narrowest VLA spectral-line bandwidths (bandwidth codes 8 and 9; see Tables 14 and 15), and restrict their observing frequencies so that only multiples of 1 MHz are used for the fluke frequencies.⁷

3.16 VLBI Observations

The VLA often participates in VLBI observations with the VLBA, and in Global Network sessions which occur three or four times per year. The VLA supports VLBI observations in either single-antenna or phased-array modes. Data are recorded on a Mark 5A disk recording system after the single-antenna or phased-array data have been passed through the VLA’s VLBA data acquisition system. At this writing, we are just completing the implementation of phasing of the EVLA antennas together with the VLA antennas, so that the phased-array VLA will contain ~ 25 antennas added in phase rather than a maximum of ~ 20 . A comprehensive document entitled ‘VLBI at the VLA’ is available on the Web – point your browser to <http://www.vla.nrao.edu/astro/> and look under ‘Proposer Information and Documentation’. Be aware that this guide is somewhat out of date, and will soon be revised.

VLBI at the VLA is overseen by Amy Mioduszewski and Mark Claussen. Either can be consulted for general information regarding matters such as phased-array or single-dish observations, or calibration of the VLA for VLBI. However, most VLBI projects involving the VLA, whether run during or outside of a Network session, will be assigned an AOC contact by the Scheduler. Queries from an observer concerning specific information about a specific project should be directed to the AOC contact assigned to the project. If the project’s principal investigator or a co-investigator is an AOC employee, then that person will be assumed to be the AOC contact.

See Section 4.15 for information on absentee observing.

3.17 Snapshots

The two-dimensional geometry of the VLA allows a snapshot mode whereby short observations can be used to image relatively bright unconfused sources. This mode is ideal for survey work where the sensitivity requirements are modest. Due to confusion by background sources, use of snapshots is not recommended at 90 cm or 400 cm.

Single snapshots with good phase stability should give dynamic ranges of a few hundred. Note that because the snapshot synthesized beam contains high sidelobes, the effects of background confusing sources are much worse than for full syntheses, especially at 20 cm in the **D** configuration, for which a single snapshot will give a limiting noise of about 0.2 mJy. This level can be reduced by taking multiple snapshots separated by at least one hour. Use of the AIPS program **IMAGR** is necessary to remove the effects of background sources. Before considering snapshot observations at 20 cm, users should first determine if the goals desired can be achieved with the existing FIRST (**B** configuration) or NVSS (**D** configuration, all-sky) surveys. Both surveys can be accessed from the NRAO website, at: <http://www.vla.nrao.edu/astro/prop/largeprop/> .

⁷Note that the phase jumps as a function of Fluke settings are still under investigation; please see <http://www.vla.nrao.edu/astro/guides/evlareturn/> for the latest information.

3.18 Shadowing and Cross-Talk

Observations at low elevation in the **C** and **D** configurations will commonly be affected by shadowing. It is strongly recommended that all data from a shadowed antenna be discarded. This will automatically be done within the AIPS task `FILLM` when using the default inputs. Note that for versions of AIPS up through early incarnations of 31DEC01, `FILLM` is ignorant of antennas in other subarrays, or antennas which are out of the array, so flagging of antennas shadowed by antennas in other subarrays will not occur. For the final 31DEC01 AIPS and all subsequent versions, `FILLM` is smart enough to know about all antennas in all VLA subarrays.

Cross-talk is an effect in which signals from one antenna are picked up by an adjacent antenna, causing an erroneous correlation. At 20 cm, this effect is important principally in the **D** configuration. At 90 cm, **C** and even **B** configurations can also be affected. And at 400 cm, all configurations show strong cross-talk on many baselines. Careful editing is necessary to identify and remove this form of interference. For the 90 and 400 cm bands, use of the spectral line modes is strongly recommended to allow detection and removal of these contaminating signals.

3.19 Combining Configurations and Mosaicing

Any single VLA configuration will allow accurate imaging up to a scale approximately 30 times the synthesized beam. Objects larger than this will require multiple configuration observations. For continuum projects, observers only need ensure that the frequencies used are similar for each configuration. It is not necessary that they be identical, but differences greater than 50 MHz could cause errors due to spectral index gradients. The different configurations may employ different bandwidths – indeed, this is often required to prevent bandwidth smearing (chromatic aberration). Objects larger than the primary antenna pattern may be mapped through the technique of interferometric mosaicing. Time-variable structures (such as the nuclei of radio galaxies and quasars) cause special, but manageable, problems. See the article by Mark Holdaway in reference 2 for more information.

3.20 Pulsar Observing

The hardware for pulsar-specific observing modes at the VLA is no longer supported, and potential proposers should consider making use of telescopes that are more suitable for pulsar timing observations. The VLA is most fruitfully used for pulsar observations in its more traditional observing modes, accepting the signal/noise penalty that is paid by accepting data at all times rather than gating the correlator synchronously with the pulsar. The EVLA will offer significant new pulsar observing capability with its new correlator, starting in around 2010.

3.21 Observing High Flux Density Sources – Special Corrections

The VLA correlator is a digital device, which causes a small but noticeable error in the calculation of the correlation coefficient when this coefficient is high. A recent change to the AIPS program `FILLM` now enables an approximate correction of this error when observations are taken in the continuum mode. Users may wish to apply this correction (commonly known as the ‘Van Vleck’ correction) when observing relatively unresolved objects with flux densities exceeding about 100 Jy (depending on band). Unfortunately, no correction for this effect for data taken in the spectral line modes is yet available.

3.22 Using VLA and EVLA Antennas Together

Throughout this document, we provide some specific information that may be essential for observing with the VLA while it combines both “old” VLA antennas and retrofitted EVLA antennas. However, since this document is updated only (approximately) annually, astronomers are urged to consult <http://www.vla.nrao.edu/astro/guides/evlareturn/> for the latest information, and follow the suggestions described therein. This is critical to the successful use of the VLA-EVLA baselines,

which will encompass approximately half of the baselines of the operational VLA by late 2007 or early 2008.

4 USING THE VLA

4.1 Obtaining Observing Time on the VLA

Observing time on the VLA is available to all researchers, regardless of nationality or location of institution. There are no quotas or reserved blocks of time. The allocation of observing time on the VLA is based upon the submission of a VLA Observing Proposal using the on-line VLA proposal tool available via <http://www.vla.nrao.edu/astro/prop/vlapst/>. *Note that proposals using the old VLA L^AT_EX form are no longer accepted!* The on-line tool permits the detailed construction of a cover sheet specifying the requested observations, using a set of on-line forms, and uploading of a pdf-format scientific and technical justification to accompany the cover information.

Students planning to use the VLA for their Ph.D. dissertation may have a problem in that such dissertations are frequently composed of pieces of several short proposals which may not be suitable for combining into a single proposal for refereeing purposes. In this case, we shall accept, one per student, a ‘Plan of Dissertation Research’, of no more than 1000 words, at the time of the first proposal of the series, and which can be referred to in later proposals. The plan of dissertation research should be e-mailed to schedsoc@nrao.edu. This provides some assurance against a dissertation being seriously damaged by adverse referee comments on one component proposal, when the referees may not see the whole picture. This facility is offered to students for which VLA observations are the most important component of their planned dissertations.

The VLA is scheduled on a trimester basis, with each trimester lasting four months. The proposal deadline for a particular configuration is 5PM (1700), Eastern Time on the 1st of February, June, or October which precedes the beginning of that configuration by three months or more. (If the first of the month falls on a Saturday or Sunday, the deadline is advanced to the next Monday.) As stated in Section 2, the traditional VLA configuration rotation is expected to be modified over the next several years, during EVLA commissioning. It is not necessary to submit a proposal at the last possible deadline for a particular configuration, since all proposals will be refereed immediately following the deadline of submission, regardless of the configuration requested. Early submissions – more than one deadline in advance of the relevant configuration deadline – will benefit from referee feedback and the opportunity for revision and additional review if warranted.

All proposals are externally refereed by several experts in relevant subdisciplines (e.g. solar system, stellar, galactic, extragalactic, etc.). The referees’ comments and rating are strongly advisory to the VLA/VLBA Proposal Selection Committee, and the comments of both groups are passed on to the proposers soon after each meeting of the committee (three times yearly) and prior to the next proposal submission deadline. See <http://www.aoc.nrao.edu/epo/ad/scheduling/shtml> for a detailed description of the time allocation process.

A special refereeing process has been established for proposals requesting an unusually large amount of time – 200 hours or more for any individual NRAO telescope (or combinations thereof). Details of this process can be found via <http://www.vla.nrao.edu/astro/prop/largeprop/>.

Scheduling the telescope is a non-exact science, and because of competition, even highly rated proposals are not guaranteed to receive observing time. This is particularly true for programs that concentrate on objects in the LST ranges occupied by popular targets such as the Galactic Center or the Virgo cluster.

4.2 Rapid Response Science

The NRAO has established three categories of proposals for Rapid Response Science, which are described below and at <http://www.vla.nrao.edu/astro/prop/rapid/>. At present, Rapid Response Science is limited to a maximum of 5% of the total observing time on the VLA. All proposals for Rapid Response Science must be submitted using the standard NRAO procedures, using the

on-line proposal tool. Proposals submitted by any other means (e.g., phone calls, e-mails, faxes, word-of-mouth) will be rejected.

1. Known Transient Phenomena. These proposals will request time to observe phenomena that are predictable in general, but not in specific detail. For example, a proposal to observe the next flaring X-ray binary that meets certain criteria would be included in this category. Specific triggering criteria will be required. These proposals will be evaluated as part of the normal refereeing and scheduling process, and will be subject to the normal NRAO proposal deadlines. The proprietary period for observations of Known Transient Phenomena will be 12 months.

2. Exploratory Time. These proposals generally follow up on recent discoveries, with observations requested in advance of the period allocated at the most recent proposal deadline(s). Examples include **B** configuration proposals that follow up on **A** configuration discoveries made after the **B** configuration deadline, or a newly identified object that is a hot enough topic to warrant an image within a couple months. In general, there will not be a need for immediate scheduling with these proposals, but they may need to be observed in the current VLA configuration rather than waiting 16 months. Proposals for Exploratory Time will be evaluated by the VLA/VLBA Proposal Selection Committee, and may or may not be sent to external referees. The possibility that a proposer forgets about or misses a proposal deadline will not constitute sufficient justification for granting of observing time by this process. Notification of the dispensation of Exploratory Time proposals normally will be within two weeks of reception of the proposal; most of the accepted proposals are placed in the dynamic scheduling queue, and are not guaranteed to be observed. The proprietary period for Exploratory Time will be six months.

3. Target of Opportunity. These proposals are for true targets of opportunity—unexpected or unpredicted phenomena such as supernovae, novae, or extreme X-ray, optical, or radio flares in various types of objects. These proposals will be evaluated rapidly, with scheduling done as quickly as possible and as warranted by the nature of the transient phenomenon. Notification of the dispensation of Target of Opportunity proposals will always be within two weeks, and may be much faster, depending on the requirements of the proposed observation. The proprietary period for Targets of Opportunity will be decided on a case-by-case basis, and will in no instances be longer than six months.

4.3 Data Analysts and General Assistance

General assistance of all kinds is available through the data analysts. They can be considered to be advocates for all VLA users, and should be consulted first when you encounter any problem. Note that they are not available to perform remote data calibration. The e-mail address for all the data analysts is: analysts@nrao.edu.

4.4 Observing File Preparation

To use the VLA, an observing file must be prepared and submitted to VLA Operations. This file may be generated by the NRAO-supplied program `JObserve`, which is a GUI-based version of the older `OBSERVE` program, offering a more modern graphical user interface without `OBSERVE`'s keypad mapping problems. New capabilities (such as support for VLA observing using the Pie Town antenna) have been added to `JObserve` only.

After your file is prepared, e-mail it to the operators at observe@nrao.edu. Include the program name in the subject line. The operators always acknowledge receipt of the observing file by e-mail. If you do not receive a timely response, call the telescope operators at 505-835-7180. Please complete these operations at least two working days before your observing.

`JObserve` distributions are currently available for Solaris (Sparc) and Linux with instructions provided to allow a user to port one of these distributions to any machine which can run the Java 2 runtime environment. The latest version of `JObserve` is 1.7.4, released January 13, 2006, and it may be downloaded from <http://www.aoc.nrao.edu/software/jobserve/>.

4.5 Fixed Date and Dynamic Scheduling

Most of the observing time on the VLA is allocated as “fixed-time” observing, with the observer being given a particular sidereal date and time allocation on the VLA. However, the VLA gradually is moving toward a system in which more observations are scheduled dynamically, based on a combination of scientific priority and the expected properties of the array and the weather. In particular, all time during antenna moves and all “filler” time are scheduled dynamically. The procedure for generating observing scripts is similar to that described in Section 4.4, except that the individual scans must be specified in time durations rather than by the absolute stop time. After preparation, observe files for dynamic scheduling are e-mailed to dynsoc@nrao.edu for queueing. Since the details of dynamic scheduling are changing on a more frequent basis than this document, we refer the reader to the scheduling officers’ home page for further information; this page is located at <http://www.aoc.nrao.edu/~schedsoc/>.

4.6 The Observations and Remote Observing

Observers need not be present at the VLA to obtain VLA data. However, we encourage VLA users to come to Socorro when observing. There is no better way to interact with the data, and to calibrate and image data quickly. And coming to Socorro is the best way to benefit from discussions with staff members.

We recommend that observers who are coming to Socorro, and who intend to set up their observing files there, arrive two working days before their scheduled observations to allow sufficient time to interact with key staff members. See Section 4.12 for information on coming to and staying in Socorro.

For those who choose to process their data at home, the data can be retrieved from the VLA on-line archive after obtaining the project key from the data analysts, or the data analysts will, upon request, mail you a tape (Exabyte or DAT) containing your uncalibrated data in its original format. The AIPS task FILLM is used to load these data to disk.

4.7 Data Processing

NRAO supports the AIPS (Astronomical Image Processing System) software as its primary data-analysis package for the VLA. This portable package may be run under various flavors of Linux or Unix operating systems, as well as Mac-OS. Most observers install and use the software on their desktop computers and/or laptops to reduce their VLA data. See <http://www.aoc.nrao.edu/aips/> for more details.

NRAO is presently developing the CASA (Common Astronomy Software Applications) package, primarily for data analysis using the EVLA and ALMA. CASA is expected to be available with some user features in 2007, and as a more complete user package in 2008. See <http://casa.nrao.edu> for more information.

4.8 Travel Support for Visiting the AOC and VLA

For each observing program scheduled on an NRAO telescope, reimbursement may be requested for one of the investigators from a U.S. institution to travel to the NRAO to observe, and for one U.S.-based investigator to travel to the NRAO to reduce data. Reimbursement may be requested for a second U.S.-based investigator to either observe or reduce data provided the second investigator is a student, graduate or undergraduate. In addition, the NRAO will, in some cases, provide travel support to the Observatory for research on archival data. The reimbursement will be for the actual cost of economy airfare, up to a limit of \$1000, originating from within the U.S. including its territories and Puerto Rico. Costs of lodging in NRAO facilities can be waived for students on advance request and with the approval of the relevant site director. No reimbursement will be made for ground transportation or meals.

To qualify, the U.S. investigator must not be employed at a Federally Funded Research and Development Center (FFRDC) or its sponsoring agency. The NSF maintains a master government list of some FFRDCs at <http://www.nsf.gov/statistics/nsf06316/>.

To claim this reimbursement, obtain an expense voucher from Terry Romero in Room 330 in the AOC.

4.9 Student Assistance for Data Reduction Visits to the AOC

Students visiting the Array Operation Center for the purposes of working on a VLA or VLBA observing program may be eligible to have their lodging expenses in the NRAO guest house covered by NRAO. To qualify, the student must be a graduate or undergraduate enrolled at a University in the U.S., working on an approved observing program. These are the same qualifications as required for NRAO support of air travel costs described above. In addition, the duration of the visit should be between 5 and 30 days. Requests for support should be made to Claire Chandler at least 4 weeks in advance of the proposed visit. If this is a first time visit then the student should be accompanied by a collaborator on the project, or alternatively an NRAO collaborator may be requested.

4.10 Real-Time Observing

A workstation, connected to the on-line computers by an Ethernet link, is now in place at the VLA site. A special version of the AIPS task FILLM will fill VLA data into this workstation's disks in real time. Each scan is available for editing, calibration, and imaging with AIPS within a few seconds of the end of that scan. Data also can be written to a local Exabyte tape.

The real-time data pipeline also has been extended to the AOC. Any workstation at the AOC can now receive VLA data as it is produced. However, this capacity is not available beyond the AOC, as tests have given inconsistent results.

4.11 Computing at the AOC

A primary goal of the computing environment at the AOC is to allow every user full access to a workstation during his/her visit. There are 8 public workstations available at the AOC for full-time data reduction by visitors. They are dual-processor 1.7-GHz PCs running Linux.

For hardcopy, we have a number of high volume B&W laser printers, two color Postscript laser printers which can reproduce on both paper and transparencies, and one wide-bed color printer.

Visitors may reserve time on these workstations when they make their travel arrangements with the Reservationist (see Section 4.12). The reservationist's e-mail is: nmreserv@nrao.edu. Gayle Rhodes schedules all public computers.

If you require computing assistance while at the AOC, contact the help desk (e-mail to helpdesk@oc.nrao.edu, extension 7213, office 262).

For a more complete description of computing facilities at the AOC, see <http://www.aoc.nrao.edu/computing/>.

4.12 Reservations for VLA and/or AOC

Advance contact with the Reservationist (nmreserv@nrao.edu) at least 1 week prior to your visit to the NRAO/NM is required, and 2 weeks' notice is preferred, in order to optimize the logistics of room occupancy, transportation, computer load, and staff assistance. You may now book your visit to the AOC through the WWW. From the NRAO home page, press the 'Sites and Telescopes' link, then 'Socorro' link, and finally the 'Visitor's Registration Form' link.

First time visiting students will be allowed to come to the NRAO/NM for observations or data reduction only if they are accompanied by their faculty advisor, or if they have a collaborating NRAO staff member.

4.13 Staying in Socorro

Visitors to Socorro can take advantage of the NRAO Guest House. This facility contains eight single, four double, and two two-bedroom apartments, plus a lounge/kitchen, and full laundry facilities. The Guest House is located on the New Mexico Tech (NMIMT) campus, a short walk from the AOC. Reservations are made through the Reservationist (nmreserv@nrao.edu.)

4.14 Help for Visitors to the VLA and AOC

We encourage observers to come to Socorro to calibrate and image their data. This is the best way to ensure the quickest turnaround and the best results from their observing. While in Socorro, each observer will interact with members of the AOC staff in accordance with his/her level of experience and the complexity of the observing program. If requested on the original VLA application form, the visiting observer will be guided through the steps of data calibration and imaging by a prearranged staff friend or scientific collaborator. A list of staff scientists and their interests can be found at <http://www.aoc.nrao.edu/epo/AD/aoc-research.html>. The data analysts and the computer operations staff are also available for consultation on AIPS procedures and systems questions.

4.15 VLBI Remote Observing

The VLA supports absentee VLBI observations, whether conducted during, or outside of, a Global Network session. Queries from an absentee observer concerning a specific project should be directed to the AOC contact assigned to that project (see Section 3.16). VLA schedule file preparation assistance is provided by the data analysts (see Section 4.3). Absentee observers must provide the data analysts with all necessary scheduling information. For a Network project, this information is due at least two weeks before the start of the appropriate Network session. For a non-Network project, this information is due by the schedule file due date assigned by the VLBA scheduler.

Although VLA Operations fully supports absentee VLBI observing, visits by observers are welcomed and are especially encouraged if the observations are in any way atypical. Included in this category are VLBI spectral line projects regardless of recording format, and any phased-array VLBI projects for which radio frequency interference is expected.

For more information, consult ‘VLBI at the VLA’.

4.16 On-Line Information about the NRAO and the VLA

NRAO-wide information is available on the World Wide Web through your favorite Web browser at URL <http://www.nrao.edu>, and information specific to astronomers using the VLA may be found at <http://www.vla.nrao.edu/astro/>. We strongly recommend usage of this on-line service, which is regularly updated by the NRAO staff.

5 MISCELLANEOUS

5.1 VLA Archive Data

The VLA archive contains all VLA data since observing started in 1976. The entire archive is now on disk, and is available via the web. A catalog describing these observations can be accessed from <http://archive.nrao.edu/archive/>. Data-base searches may be made based on a large number of user-specified criteria, and automatic downloading of the data via standard `ftp` protocols. With the exception of some rapid response and large proposals, VLA data associated with a given proposal normally are restricted to proprietary use by the proposing team for a period of 12 months from the date of the last observation in a proposal.⁸ Proprietary data may be downloaded by the observing team by making use of the project key (see Section 4.6).

⁸Data taken more than 12 months previously may still be proprietary, if additional data for the same proposal have been taken within the last 12 months.

5.2 Publication Guidelines

5.2.1 Acknowledgement to NRAO

Any papers using observational material taken with NRAO instruments (VLA or otherwise) or papers where a significant portion of the work was done at NRAO, should include the following acknowledgement to NRAO and NSF:

The National Radio Astronomy Observatory is a facility of the National Science Foundation operated under cooperative agreement by Associated Universities, Inc.

5.2.2 Dissertations

Students whose dissertations include observations made with NRAO instruments are expected to provide copies of, or links to, their theses for inclusion and maintenance at the NRAO library. These will be catalogued and made available via the NRAO library catalogue. If a paper copy (unbound is acceptable), it may be submitted to the AOC Librarian who will send it to Charlottesville for cataloguing.

5.2.3 Preprints

NRAO requests that you submit the `astro-ph` link or an electronic copy of any accepted papers that include observations taken with any NRAO instrument or have NRAO author(s) to the Observatory Librarian. For further information, contact the Librarian in Charlottesville (`library@nrao.edu`) or read the instructions on the web page at <http://www.nrao.edu/library/preprints.shtml>.

5.2.4 Reprints

NRAO no longer distributes reprints, but will purchase the minimum number of reprints for NRAO staff members. The NRAO does not want reprints, and will not pay for any reprint costs for papers with no NRAO staff author.

5.2.5 Page Charge Support

The following URL contains complete information on the observatory's policy regarding page charge support: http://www.cv.nrao.edu/library/page_charges.html. The following is a summary:

- When requested, NRAO will pay the larger of the following:
 - 100% of the page charge share for authors at a U.S. scientific or educational institute reporting original results made with NRAO instrument(s). See the VLA web pages for more details.
 - 100% of the page charge share for NRAO staff members.
- Page charge support is provided for publication of color plates.
- To receive page charge support, authors must comply with all of the following requirements:
 - Include the NRAO footnote in the text (see Section 5.2.1).
 - Send the `astro-ph` link or an electronic copy of the paper upon acceptance or posting on `astro-ph` to the Observatory Librarian (`library@nrao.edu`), with the request for page charge support. The Librarian will respond with the amount covered (based on the NRAO page charge policy) and will request the page charge form, with manuscript information completed, via fax (434-296-0278) or e-mail (`library@nrao.edu`). For questions, contact the Observatory Librarian at 434-296-0254.

6 DOCUMENTATION

Documentation for VLA data reduction, image making, observing preparation, etc., can be found in various manuals. Most current manuals are available on-line via the World Wide Web (see Section 4.16). Those manuals marked by an asterisk (*) can be mailed out upon request, or are available for downloading from the NRAO website. Direct your requests for mailed hardcopy to Gayle Rhodes. Many other documents of interest to the VLA user, not listed here, are available from our website.

1. PROCEEDINGS FROM THE 1988 SYNTHESIS IMAGING WORKSHOP: Synthesis theory, technical information and observing strategies can be found in: ‘Synthesis Imaging in Radio Astronomy’. This collection of lectures given in Socorro in June 1988 has been published by the Astronomical Society of the Pacific as Volume 6 of their Conference Series.
2. PROCEEDINGS FROM THE 1998 SYNTHESIS IMAGING WORKSHOP: This is an updated and expanded version of Reference 1, taken from the 1998 Synthesis Imaging Summer School, held in Socorro in June, 1998. These proceedings are published as Volume 180 of the ASP Conference Series.
3. INTRODUCTION TO THE NRAO VERY LARGE ARRAY (Green Book): This manual has general introductory information on the VLA. Topics include theory of interferometry, hardware descriptions, observing preparation, data reduction, image making and display. Major sections of this 1983 manual are now out of date, but it nevertheless remains the best source of information on much of the VLA. Copies of this are found at the VLA and in the AOC, but no new copies are available. Much of this document is available for downloading through the NRAO’s website.
4. *A SHORT GUIDE FOR VLA SPECTRAL LINE OBSERVERS: This is an important document for those wishing to carry out spectral- line observations with the VLA. The revised, 1995 version is still fairly current.
5. *AIPS COOKBOOK: The ‘Cookbook’ description for calibration and imaging under the AIPS system can be found near all public workstations in the AOC. The latest version has expanded descriptions of data calibration imaging, cleaning, self- calibration, spectral line reduction, and VLBI reductions. See <http://www.aoc.nrao.edu/aips/cook.html> .
6. *GOING AIPS: This is a two-volume programmers manual for those wishing to write programs under AIPS. It is now somewhat out of date. See <http://www.aoc.nrao.edu/aips/aipsdoc.html#GOAIPS> .
7. *VLA CALIBRATOR MANUAL: This manual contains the list of VLA Calibrators in both 1950 and J2000 epoch and a discussion of gain and phase calibration, and polarization calibration. See <http://www.vla.nrao.edu/astro/calib/manual/> .
8. *VLBI AT THE VLA. Everything you ever wanted to know about VLBI at the VLA. Presently somewhat out of date, but with a new revision expected in 2007. See <http://www.vla.nrao.edu/astro/guides/vlbivla/current/> .
9. *The Very Large Array: Design and Performance of a Modern Synthesis Radio Telescope, Napier, Thompson, and Ekers, Proc. of IEEE, 71, 295, 1983.
10. *OBSERVE, A GUIDE FOR SPECTRAL LINE OBSERVERS. A tutorial manual for observers, with special emphasis on spectral line applications.
11. *HIGH FREQUENCY OBSERVING GUIDE. A web-based manual with a great deal of information for users about observing with the VLA 0.7 cm and 1.3 cm observing systems. See <http://www.vla.nrao.edu/astro/guides/highfreq/> .
12. *VLA MEMO SERIES. See <http://www.vla.nrao.edu/memos/> .
13. *EVLA MEMO SERIES. See <http://www.aoc.nrao.edu/evla/memolist.shtml> .

7 KEY PERSONNEL

Table 16 gives the telephone extensions and AOC room numbers of personnel who are available to assist VLA users. In most cases the individuals have responsibilities or special knowledge in certain areas as noted in the right hand column. You also may contact any of these people through E-mail, as noted at the end of the table.

Table 16: Key VLA Personnel

| Name | Phone | Room | Notes |
|---------------------|-------|---------|---|
| Lori Appel | 7310 | 340 | Scheduling administrator |
| John Benson | 7399 | 366 | Data archive |
| Walter Brisken | 7133 | 301 | Pulsars; EVLA calibration |
| Bryan Butler | 7261 | 344 | EVLA Computing Division Head; Q and K band |
| Claire Chandler | 7365 | 360 | Scientific Services Division Head; Q and K band |
| Barry Clark | 7268 | 308 | Scheduling |
| Mark Claussen | 7284 | 268 | Spectral line; CASA interface |
| Ed Fomalont | | CV | Calibration/imaging service; polarization |
| Dale Frail | 7338 | 332 | Time allocation; visitor programs |
| Miller Goss | 7267 | 256 | Spectral line |
| Eric Greisen | 7236 | 210 | AIPS head |
| Helpdesk | 7213 | 262 | Computer Helpdesk |
| Leonid Kogan | 7383 | 312 | AIPS |
| Mark McKinnon | 7273 | 326 | EVLA Project Manager |
| Joe McMullin | 7327 | 368 | CASA project manager |
| Dan Mertely | 7128 | VLA-128 | RFI monitoring and mitigation |
| Amy Mioduszewski | 7263 | 367 | AIPS; VLA calibrator models; VLBI |
| Steve Myers | 7294 | 376 | VLA calibration; polarization |
| Frazer Owen | 7304 | 320 | High dynamic range; wide-field imaging |
| Peggy Perley | 7214 | 282 | VLA/VLBA Head of Operations |
| Rick Perley | 7312 | 362 | EVLA Project Scientist; flux calibration |
| Gayle Rhodes | 7245 | 267 | Documentation; computer assignments |
| James Robnett | 7226 | 258 | Computing Infrastructure Division Head |
| Terry Romero | 7315 | 330 | Visitor support |
| Michael Rupen | 7248 | 206 | EVLA scientific software; spectral line |
| Debra Shepherd | 7398 | 266 | Mosaicing |
| Lorant Sjouwerman | 7332 | 367 | VLA Pipeline |
| Ken Sowinski | 7299 | 375 | On-line systems |
| Meri Stanley | 7238 | 204 | Lead data analyst |
| Jim Ulvestad | 7300 | 336 | VLA/VLBA Assistant Director |
| Gustaaf van Moorsel | 7396 | 348 | Spectral line; post-processing software |
| Christine Wingenter | 7357 | 218 | NRAO reservationist |
| Stephan Witz | 7335 | 316 | JObserve |
| Joan Wrobel | 7392 | 302 | VLA/VLBA scheduling; proposal submission tool |
| Wes Young | 7337 | 378 | Real-time observing |

Note: You may e-mail any of the above individuals by addressing your message to ‘first initial last name’@nrao.edu. Thus, you may contact Joanne Astronomer at: ‘jastrono@nrao.edu’. The name is truncated to eight characters. The listed four-digit numbers are sufficient for calls made from within the AOC. If you are calling from the U.S. or Canada, the 4-digit numbers must be preceded with: 505-835. If you are calling from outside the U.S. or Canada, the 4-digit numbers must be preceded with 1-505-835. The VLA control room number is: 505-835-7180. The AOC’s front-desk number is: 505-835-7000.

8 Acknowledgments

Over the VLA history of more than 25 years, many individuals have contributed to this document by writing sections, editing previous versions, commenting on draft material, and implementing the capabilities described herein. We thank all these contributors for their efforts. The listed editors of the present version of this document are the editors of the most recent versions, and thus are the best individuals for readers to contact if they should have questions on the material, or suggestions that would enhance the clarity of this guide.